Thank you Dr. Fred Leve and Dr. Fariba Fahroo

Data-guided Learning and Control of Higher Order Structures

Indika Rajapakse, Anthony Bloch: University of Michigan

Amit Surana: Raytheon Technologies Research Center

Graduate Students: Joshua Pickard, Cooper Stansbury

2024 Dynamical Systems and Control Theory Program Review

LAB 2024: Team and Technology

Oxford Nanopore Sequencing

MinION

GridION

PromethION 2

The BAB robotic arm

BAB Pick n' Place tool (i.e., the grippers)

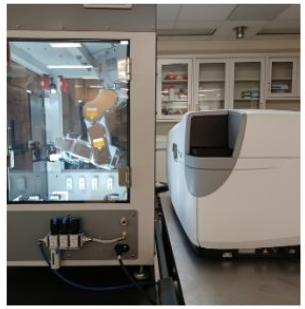

The BAB and Zeiss Celldiscoverer 7

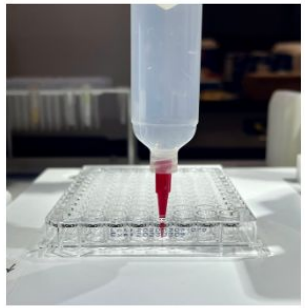

BAB Printing Tool used to automate a wound healing assay

University Research Instrumentation Program (DURIP), 2019 and 2022
Air Force Office of Scientific Research (Dr. Fred Leve)








Industrial Collaborators

Jay Hoying
Advanced Solutions

Lakmal Jayasinghe
Oxford Nanopore Technologies

Amit Surana
Raytheon Technologies

Technology Transfer to Startup: iReprogram Inc.

DURIP: Automation in the LAB

Live Cell Imaging

BAB

ONT Sequencer

Live Streaming

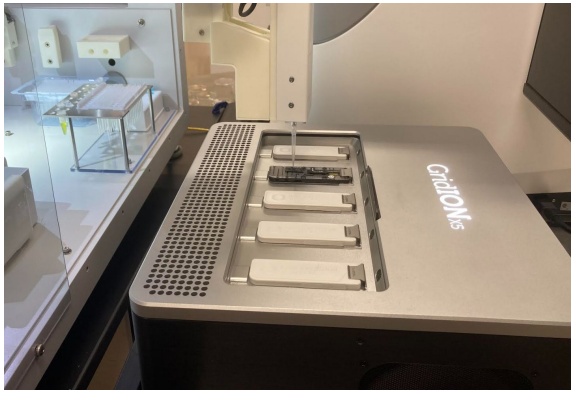

DURIP: Automation in the LAB

https://drive.google.com/file/d/1uUcQvRaHXQamtOix5xneZPXNFABYLd7z/view?usp=sharing

Current Project

Objective: Develop a data-guided framework for learning and control of higher order structure, function, and dynamics in complex systems. This would provide a new approach for understanding and intervention/control in complex systems such as cell reprogramming toward accelerated wound healing or disease recovery.

Outline

Completed

1. **Observability of Hypergraphs** (continuation)
    a. Pickard, J., Surana, A., Bloch, A. and Rajapakse, I., 2023, December. **Observability of hypergraphs**. In *2023 62nd IEEE Conference on Decision and Control (CDC)* (pp. 2445-2451). IEEE.
    b. Pickard, J., Stansbury, C., Surana, A., Rajapakse, I. and Bloch, A., 2024. **Geometric Aspects of Observability of Hypergraphs**. In 2024 *IFAC LHMNC. arXiv preprint arXiv:2404.07480*.
2. **Kronecker Products for Tensors and Hypergraphs** (continuation)
    a. Pickard, J., Chen, C., Stansbury, C., Surana, A., Bloch, A., and Rajapakse, I. (2023). **Kronecker Product of Tensors and Hypergraphs: Structure and Dynamics**. *in press at SIAM Journal on Matrix Analysis and Applications*
3. **Dynamic Biomarker Selection**
    a. Pickard, J., Stansbury, C., Surana, A., Bloch, A. and Rajapakse, I., 2024. **Biomarker Selection for Adaptive Systems**. *arXiv preprint arXiv:2405.09809*.
4. **Cellular Reprogramming of HSCs**
    a. Stansbury, C., Cwycyshyn, J., Pickard J., Meixner W., Rajapakse I., and Muir L.A., 2024, **Data-guided direct reprogramming of human fibroblasts into the hematopoietic lineage**. *bioRxiv preprint*

Outline

Ongoing

1. **Large, directed, non-uniform hypergraphs**
2. **A Programmable Platform for Probing Cellular Dynamics**
    a. Cwycyshyn, J., Stansbury, C., Meixner, W., Hoying, J.B., Muir, L.A. and Rajapakse, I., 2023. **Automated In Vitro Wound Healing Assay**. *bioRxiv*, pp.2023-12.
    b. Fabricating two-cell system
3. **Data: Single Cell Pore-C** (higher order structures in the human genome)
    a. Hypergraph Core!
4. **Digital Biology**: In-silico testing Data-guide Control using HWG and geneformer (joint project with NVIDIA)
    a. Pickard, J., Choi, M., Oliven, N., Stansbury, C., Velasquez, A., Gorodetsky, A., and Rajapakse, I. **BRAD: Retrieval-Augmented Generation for Bioinformatics**. *in preparation*

Ongoing and Future Directions

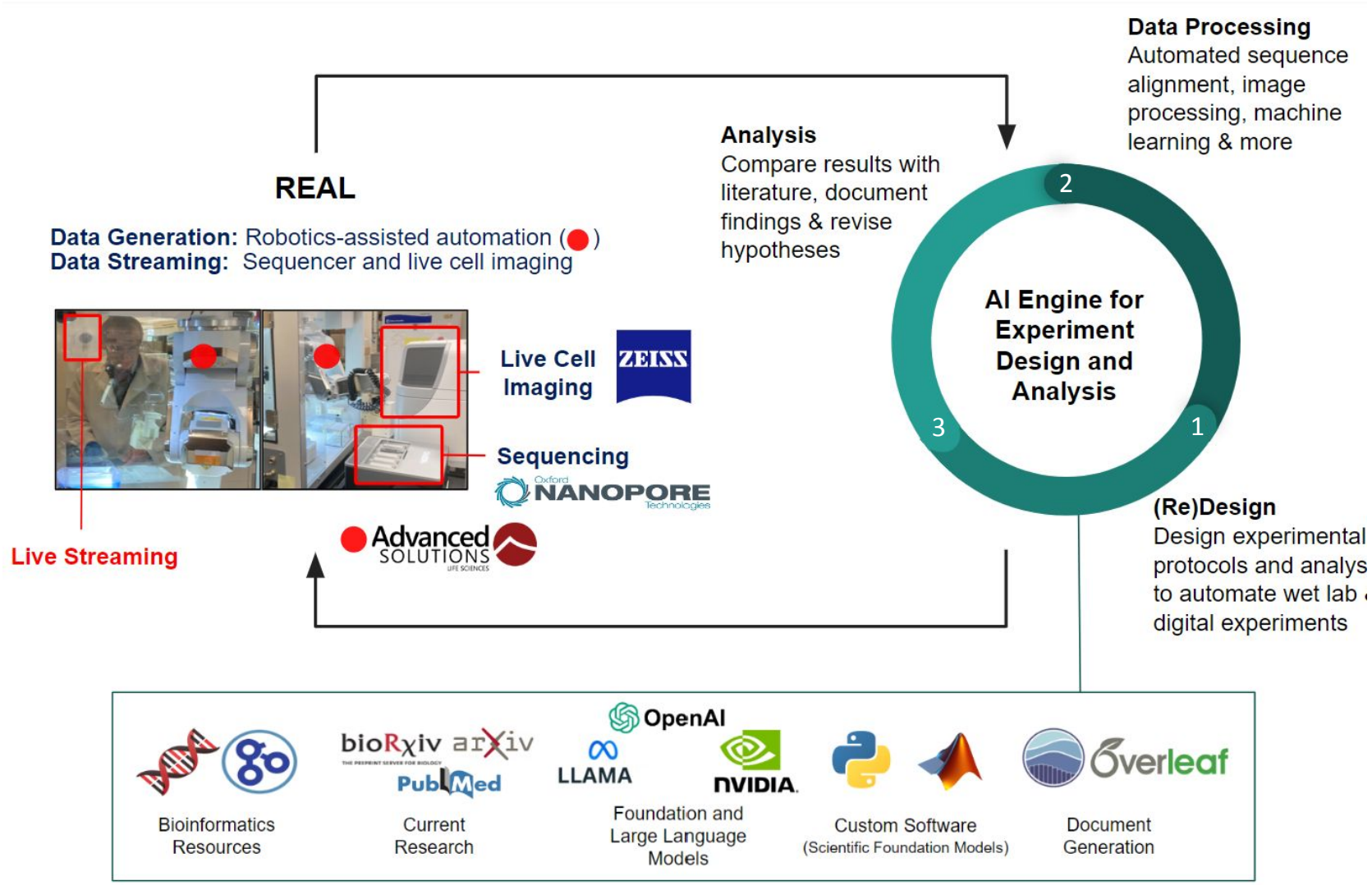

Pickard, J., Choi, M., Oliven, N., Stansbury, C., Velasquez, A., Gorodetsky, A., and Rajapakse, I. **BRAD: Retrieval-Augmented Generation for Bioinformatics**. *in preparation*

Observability of Hypergraphs (continued from 2023)

Observability: Does data uniquely determine the system state?

Hypergraphs have multi-way interactions

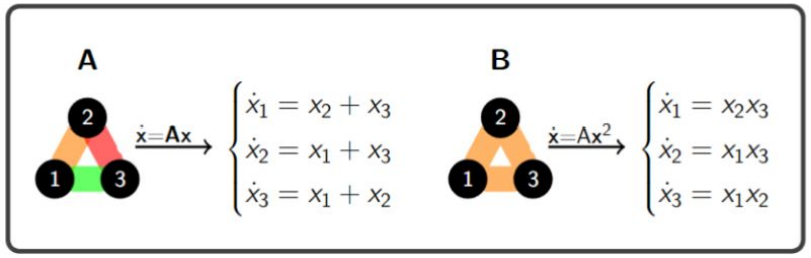

Polynomial Dynamics with Linear Observations

$$\Sigma \begin{cases} \dot{\mathbf{x}} &= \mathbf{f}(\mathbf{x}) = \mathbf{A}\mathbf{x}^{k-1} \\ \mathbf{y} &= \mathbf{g}(\mathbf{x}) = \mathbf{C}\mathbf{x}, \end{cases}$$

Homogeneous

2023 62nd IEEE Conference on Decision and Control (CDC)
December 13-15, 2023. Marina Bay Sands, Singapore

Observability of Hypergraphs

Joshua Pickard, Amit Surana, Anthony Bloch, and Indika Rajapakse

***Abstract*— In this paper we develop a framework to study observability for uniform hypergraphs. Hypergraphs, being extensions of graphs, allow edges to connect multiple nodes and unambiguously represent multi-way relationships which are ubiquitous in many real-world networks. We extend the canonical homogeneous polynomial or multilinear dynamical system on uniform hypergraphs to include linear outputs, and we derive a Kalman-rank-like condition for assessing the local weak observability. We propose an exact techniques for determining the local observability criterion, and we propose a greedy heuristic to determine the minimum set of observable nodes. Numerical experiments demonstrate our approach on several hypergraph topologies and a hypergraph representations of neural networks within the mouse hypothalamus.**

systems, we rely on estimations of the plant state based solely on the plant output or the measurements collected from its sensors. This finds various applications, such as monitoring chemical reactions network or understanding the spread of information or a disease within a community. In the context of networked systems, two fundamental questions arise:

- (Q1) Is a set of sensor nodes sufficient to render a network observable?
- (Q2) What is the minimum set of nodes to render a network observable?

Observability of network systems has been extensively studied from several perspectives; see [12] and references

IEEE CDC (2023)

Non-homogeneous

Geometric Observability of Hypergraphs

Joshua Pickard[a*], Cooper Stansbury[a], Amit Surana[b],
Indika Rajapakse[ac], and Anthony Bloch[c]
[a]Department of Computational Medicine and Bioinformatics, University of Michigan, Ann Arbor MI, USA
[b]RTX Technology Research Center, East Hartford, CT USA
[c]Department of Mathematics, University of Michigan, Ann Arbor MI, USA

April 12, 2024

Abstract

In this paper we consider aspects of geometric observability for hypergraphs, extending our earlier work from the uniform to the nonuniform case. Hypergraphs, a generalization of graphs, allow hyperedges to connect multiple nodes and unambiguously represent multi-way relationships which are ubiquitous in many real-world networks including those that arise in biology. We consider polynomial dynamical systems with linear outputs defined according to hypergraph structure, and we propose methods to evaluate local, weak observability.

IFAC LHMNC (2024)

Determining Observability (continued from 2023)

Observability Increases with Higher Order Interactions

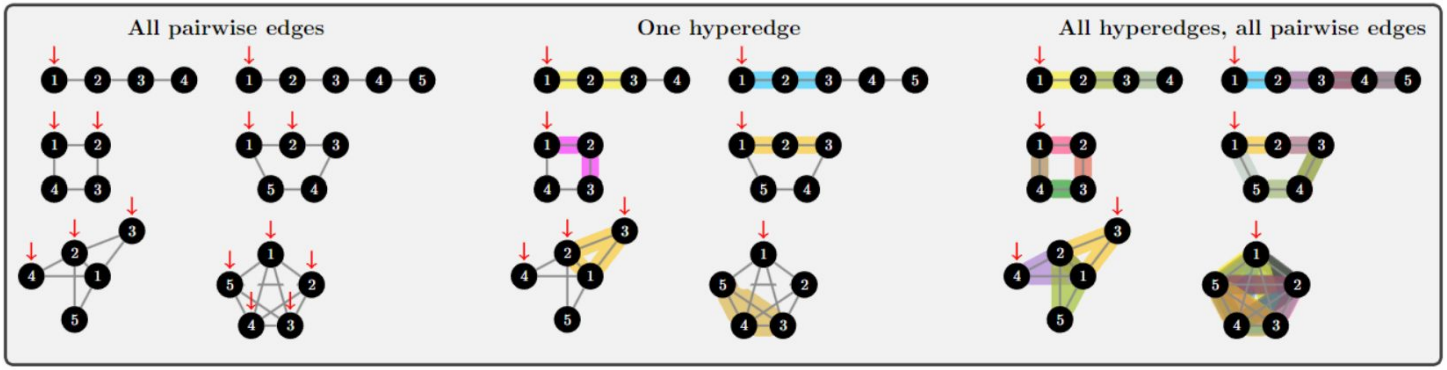

Time Series Calcium Imaging of Neurons [1]

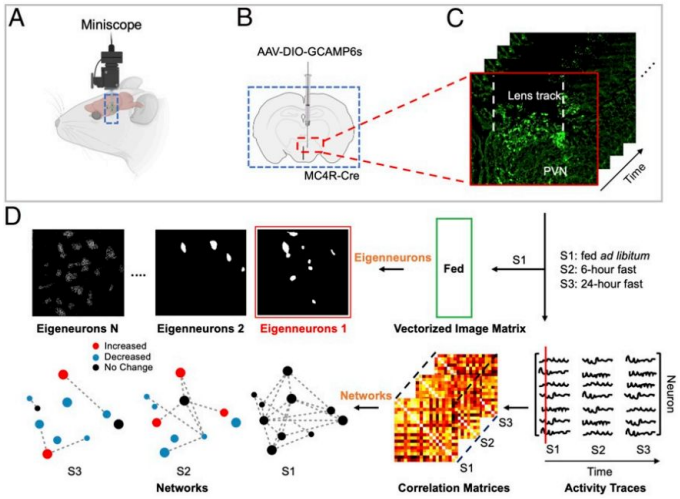

Experiment Design

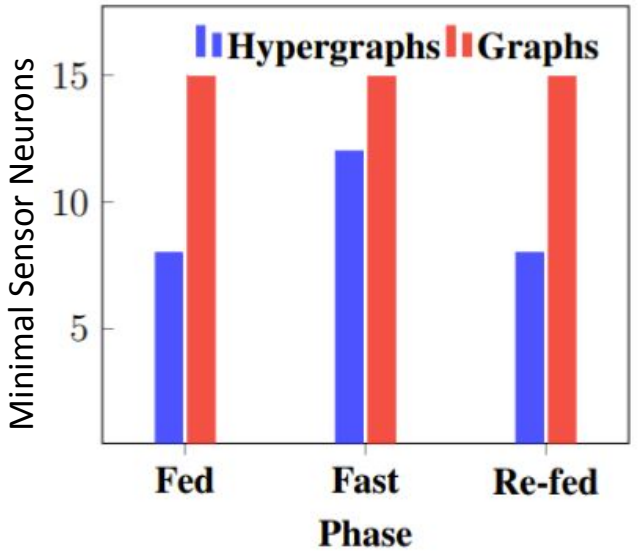

[1] Sweeney P, Chen C, Rajapakse I, Cone R. "**Network Dynamics of Hypothalamic Feeding Neurons.**" *Proceedings of the National Academy of Sciences*, 118.14 (2021)

Kronecker Products for Higher Order Systems (continued from 2023)

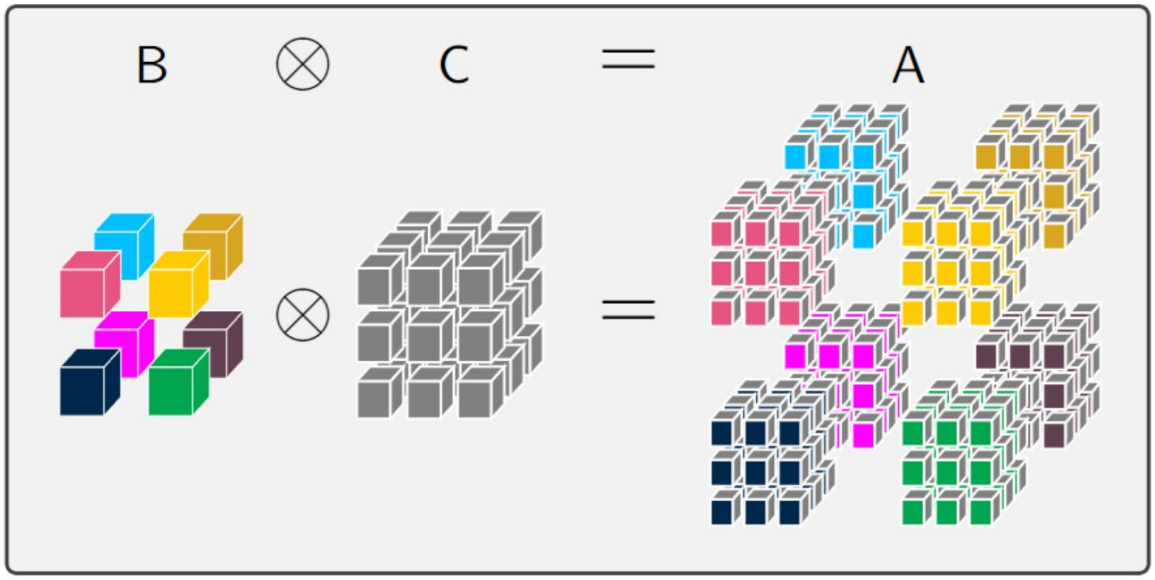

KRONECKER PRODUCT OF TENSORS AND HYPERGRAPHS: STRUCTURE AND DYNAMICS

JOSHUA PICKARD*, CAN CHEN†, COOPER STANSBURY‡, AMIT SURANA§, ANTHONY BLOCH¶, AND INDIKA RAJAPAKSE‖

Abstract. Hypergraphs and graph products extend traditional graph theory by incorporating multi-way and coupled relationships, which are ubiquitous in real-world systems. While the Kronecker product, rooted in matrix analysis, has become a powerful tool in network science, its application has been limited to pairwise networks. In this paper, we extend the coupling of graph products to hypergraphs, enabling a system-theoretic analysis of network compositions formed via the Kronecker product of hypergraphs. We first extend the notion of the matrix Kronecker product to the tensor Kronecker product from the perspective of tensor blocks. We present various algebraic and spectral properties and express different tensor decompositions with the tensor Kronecker product. Furthermore, we study the structure and dynamics of Kronecker hypergraphs based on the tensor Kronecker product. We establish conditions that enable the analysis of the trajectory and stability of a hypergraph dynamical system by examining the dynamics of its factor hypergraphs. Finally, we demonstrate the numerical advantage of this framework for computing various tensor decompositions and spectral properties.

Key words. Tensor Kronecker Product, hypergraph products, tensor decomposition, tensor eigenvalues, multilinear system, block tensors

AMS subject classifications. 15A69, 05C65

SIAM SIMAX, *to appear*

Kronecker Products for Tensor Calculations

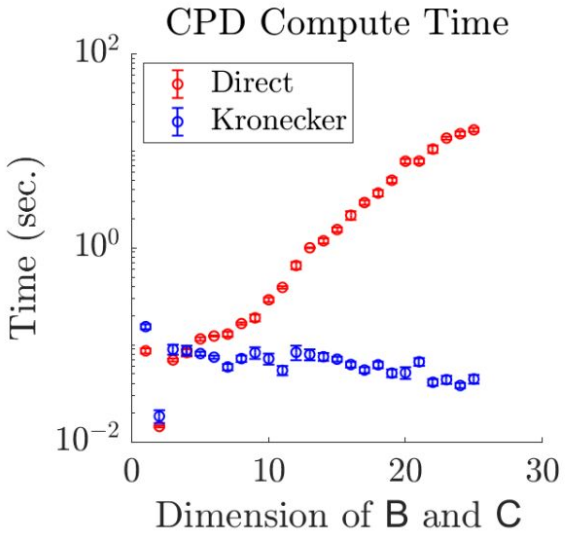

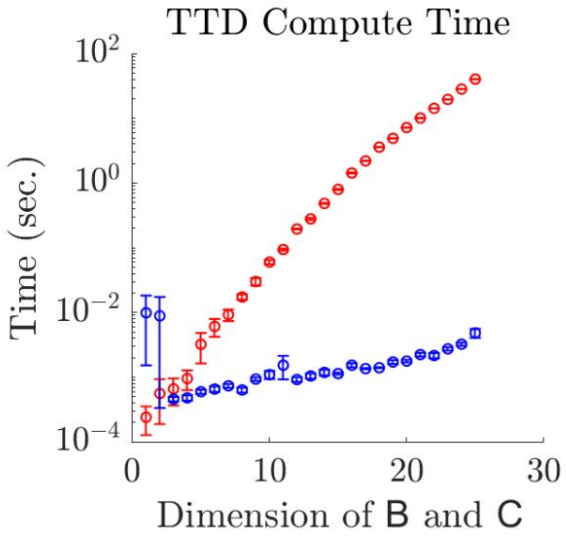

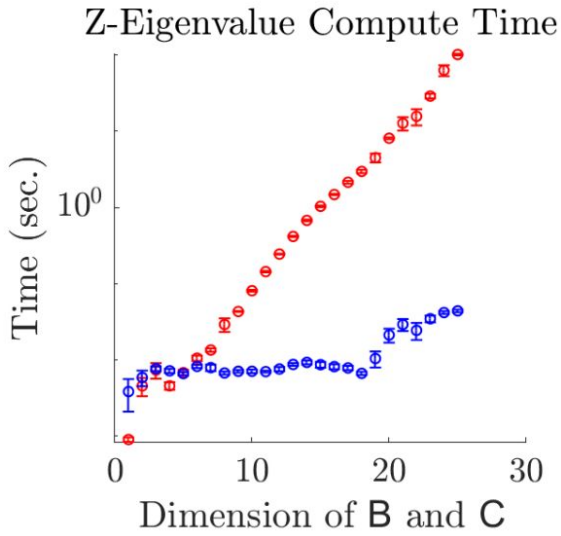

Canonical Polyadic Decomposition (CPD)

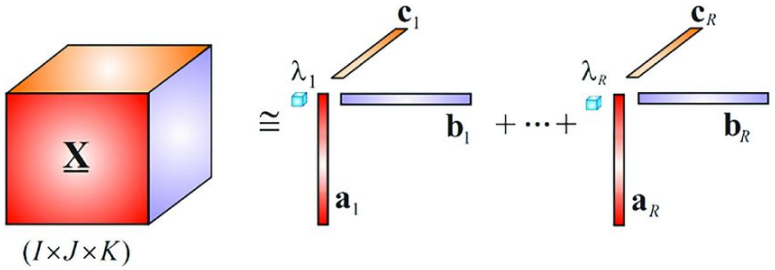

Tensor Train Decomposition (TTD)

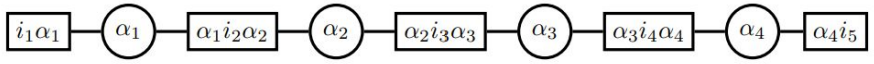

Z-Eigenvalue Problem

$$\mathcal{T}\mathbf{x}^{k-1} = \lambda\mathbf{x} \;\; and \;\; \mathbf{x}^\top\mathbf{x} = 1$$

Kronecker Products for Polynomial Dynamics

Stability of polynomial dynamical systems can be determined from Kronecker factors

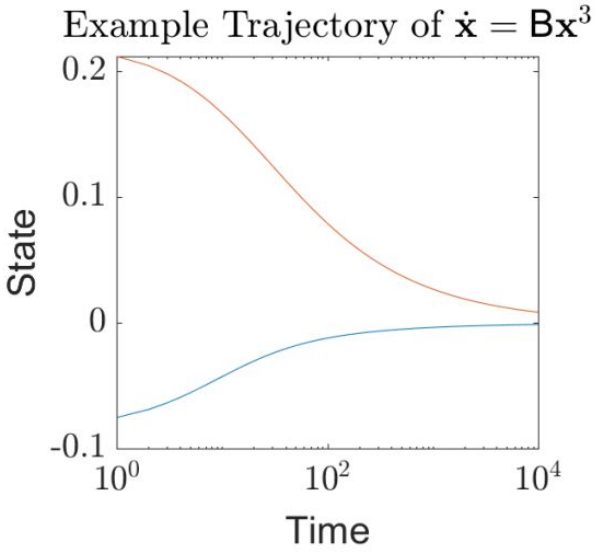

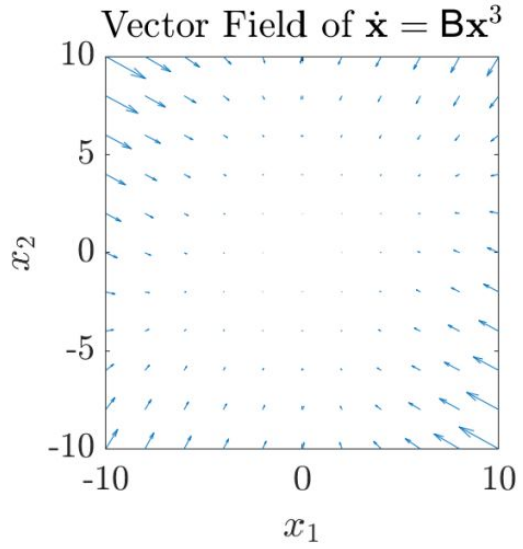

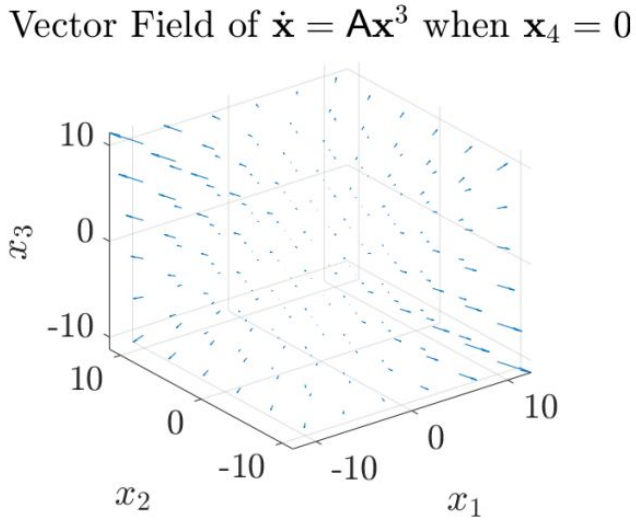

Stable 3rd Order Polynomial

$$\begin{cases} \dot{x}_1 &= -1.2593\mathbf{x}_1^3 + 1.6630\mathbf{x}_1^2\mathbf{x}_2 - 1.5554\mathbf{x}_1\mathbf{x}_2^2 - 0.1386\mathbf{x}_2^3 \\ \dot{x}_2 &= 0.5543\mathbf{x}_1^3 - 1.5554\mathbf{x}_1^2\mathbf{x}_2 - 0.4158\mathbf{x}_1\mathbf{x}_2^2 - 0.7036\mathbf{x}_2^3 \end{cases},$$

Tensor Representation

$$\frac{d\mathbf{x}}{dt} = \mathsf{B}\mathbf{x}^3$$

$$\mathsf{B}_{::11} = \begin{pmatrix} -1.2593 & 0.5534 \\ 0.5543 & -0.5185 \end{pmatrix} \quad \mathsf{B}_{::12} = \begin{pmatrix} 0.5543 & -0.5185 \\ -0.5185 & -0.1386 \end{pmatrix}$$

$$\mathsf{B}_{::21} = \begin{pmatrix} 0.5543 & -0.5185 \\ -0.5185 & -0.1386 \end{pmatrix} \quad \mathsf{B}_{::11} = \begin{pmatrix} -0.5185 & -0.1386 \\ -0.1386 & -0.7037 \end{pmatrix}$$

Kronecker Coupled System

$$\frac{d\mathbf{x}}{dt} = \mathsf{A}\mathbf{x}^3 \text{ where } \mathsf{A} = \mathsf{B} \otimes \mathsf{B}$$

Adaptive Sequencing Technology

nature

Explore content ⌄ About the journal ⌄ Publish with us ⌄

nature › articles › article

Article | Open access | Published: 11 October 2023

Ultra-fast deep-learned CNS tumour classification during surgery

C. Vermeulen, M. Pagès-Gallego, L. Kester, M. E. G. Kranendonk, P. Wesseling, N. Verburg, P. de Witt Hamer, E. J. Kooi, L. Dankmeijer, J. van der Lugt, K. van Baarsen, E. W. Hoving, B. B. J. Tops ✉ & J. de Ridder ✉

Nature **622**, 842–849 (2023) | Cite this article

Biomarker Selection for Adaptive Systems

Joshua Pickard[1,*], Cooper Stansbury[1], Amit Surana[2], Lindsey Muir[1], Anthony Bloch[3], and Indika Rajapakse[1,3,*]

[1]Department of Computational Medicine & Bioinformatics, University of Michigan, Ann Arbor, MI 48109
[2]RTX Technology Research Center, East Hartford, CT 06108
[3]Department of Mathematics, University of Michigan, Ann Arbor, MI 48109
[*]{jpic,indikar}@umich.edu

Abstract

Biomarkers enable objective monitoring of a given cell or state in a biological system and are widely used in research, biomanufacturing, and clinical practice. However, identifying appropriate biomarkers that are both robustly measurable and capture a state accurately remains challenging. We present a framework for biomarker identification based upon observability guided sensor selection. Our methods, Dynamic Sensor Selection (DSS) and Structure-Guided Sensor Selection (SGSS), utilize temporal models and experimental data, offering a template for applying observability theory to data from biological systems. Unlike conventional methods that assume well-known, fixed dynamics, DSS adaptively select biomarkers or sensors that maximize observability while accounting for the time-varying nature of biological systems. Additionally, SGSS incorporates structural information and diverse data to identify sensors which are resilient against inaccuracies in our model of the underlying system. We validate our approaches by performing estimation on high dimensional systems derived from temporal gene expression data from partial observations. Our algorithms reliably identify known biomarkers and uncover new ones within our datasets. Additionally, integrating chromosome conformation and gene expression data addresses noise and uncertainty, enhancing the reliability of our biomarker selection approach for the genome.

In Preparation: *arXiv* (2024)

Dynamic Sensor Selection

Experimental Setup

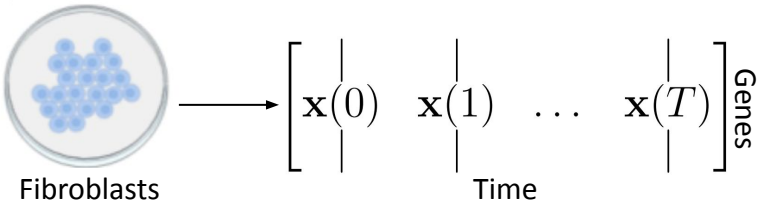

Model of Dynamics

$$\mathbf{x}(t+1) = \mathbf{A}(t)\mathbf{x}(t)$$
$$\mathbf{y}(t) = \mathbf{C}(t)\mathbf{x}(t)$$

Adaptive sequencing technologies lets us change biomarkers (sensor set) in real time

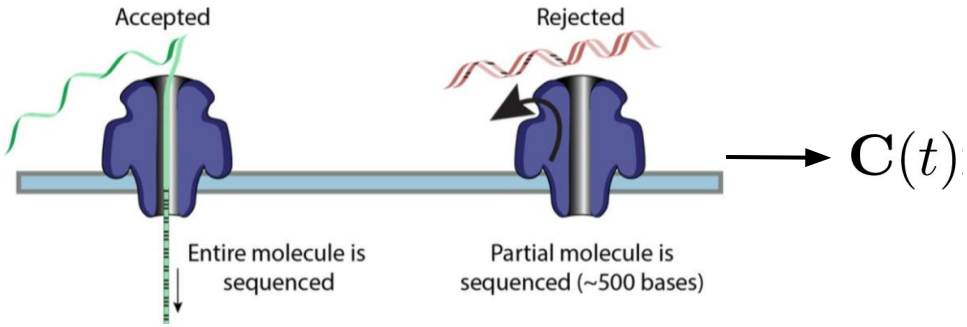

Problem: How can we change our sensors over time to maximize observability?

Output Energy Maximization

$$\max_{\mathbf{C}(t)} \mathcal{E} \text{ for all } t, \text{ where } \mathcal{E} = \sum_{t=0}^{T} \mathbf{y}(t)^\top \mathbf{y}(t)$$

Observability Gramian

$$\min_{\mathbf{C}(t)} J(\mathbb{G}_o)$$

Structure Guided Sensor Selection

Geometry of the nucleus

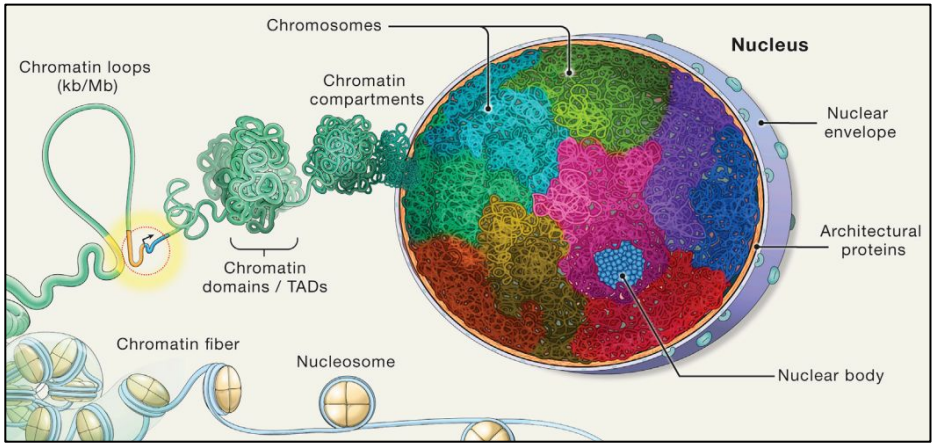

Chromosome Conformation Capture

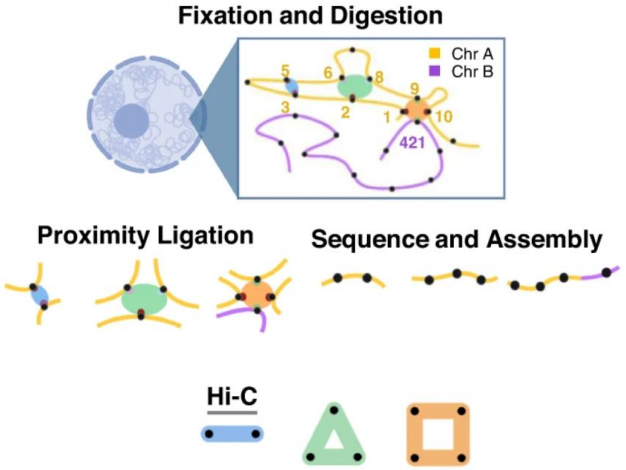

The genome is a small world

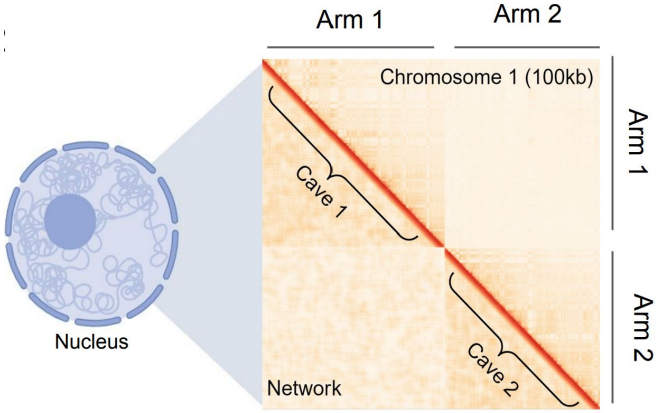

Gene-centric physical interactions

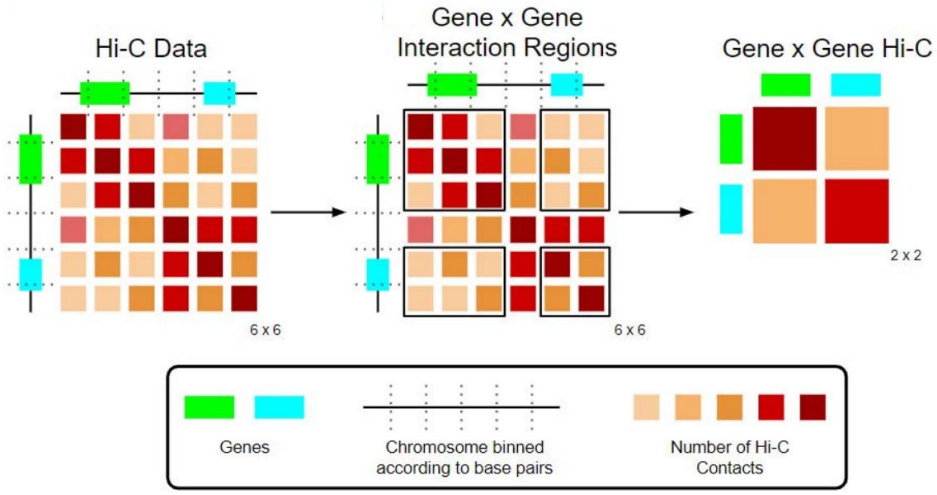

Cellular Reprogramming of Hematopoietic Stem Cells

Data-guided direct reprogramming of human fibroblasts into the hematopoietic lineage

Cooper Stansbury[1, 2], Jillian Cwycyshyn[1, 3], Joshua Pickard[1], Walter Meixner[1], Indika Rajapakse[1, 2, 4], and Lindsey A. Muir[1]

[1]Department of Computational Medicine and Bioinformatics, University of Michigan, Ann Arbor, MI 48109 USA
[2]The Michigan Institute for Computational Discovery and Engineering, University of Michigan, Ann Arbor, MI 48109 USA
[3]Department of Biomedical Engineering, University of Michigan, Ann Arbor, MI 48109 USA
[4]Department of Mathematics, University of Michigan, Ann Arbor, MI 48109 USA

August 26, 2024

Abstract

Direct reprogramming of human fibroblasts into hematopoietic stem cells (HSCs) presents a promising strategy for overcoming the limitations of traditional bone-marrow transplantation. Despite the potential of this approach, our understanding of the mechanisms driving efficient autologous cell type conversion remains incomplete. Here, we evaluate a novel algorithmically predicted transcription factor (TF) recipe - GATA2, GFIB1, FOS, REL, and STAT5A - for inducing HSC-like states from human dermal fibroblasts. Using flow cytometry and long-read single-cell RNA-sequencing, we demonstrate increased $CD34^{+}$cell populations and high transcriptomic similarity to native HSCs. Additionally, we uncover transcriptional heterogeneity at both gene and isoform levels among induced HSCs, underscoring the complexity of direct reprogramming.

In Preparation: *bioRxiv* (2024)

Cellular Reprogramming of Hematopoietic Stem Cells

LTI Model of Cellular Proliferation [1]

$$\frac{d\mathbf{x}}{dt} = \mathbf{A}(t)\mathbf{x}(t) + \mathbf{B}\mathbf{u}(t)$$

Transcription Factor (TF) Binding Sites

Application of TF Control Signal $\mathbf{u}(t)$

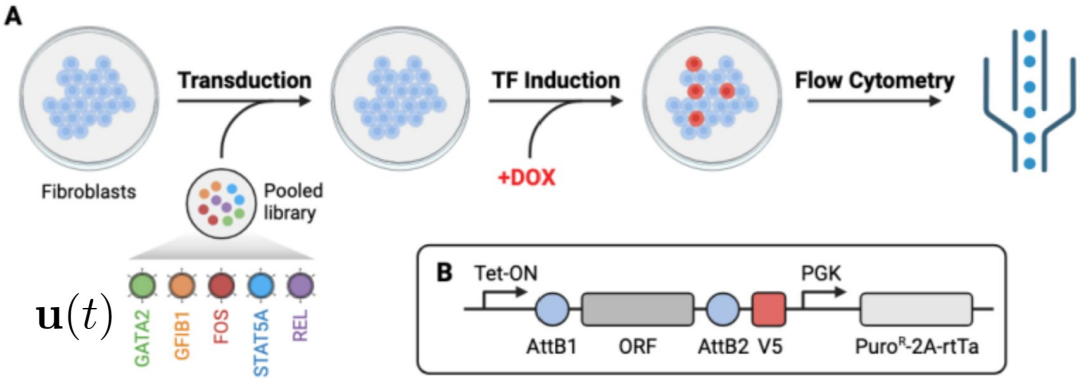

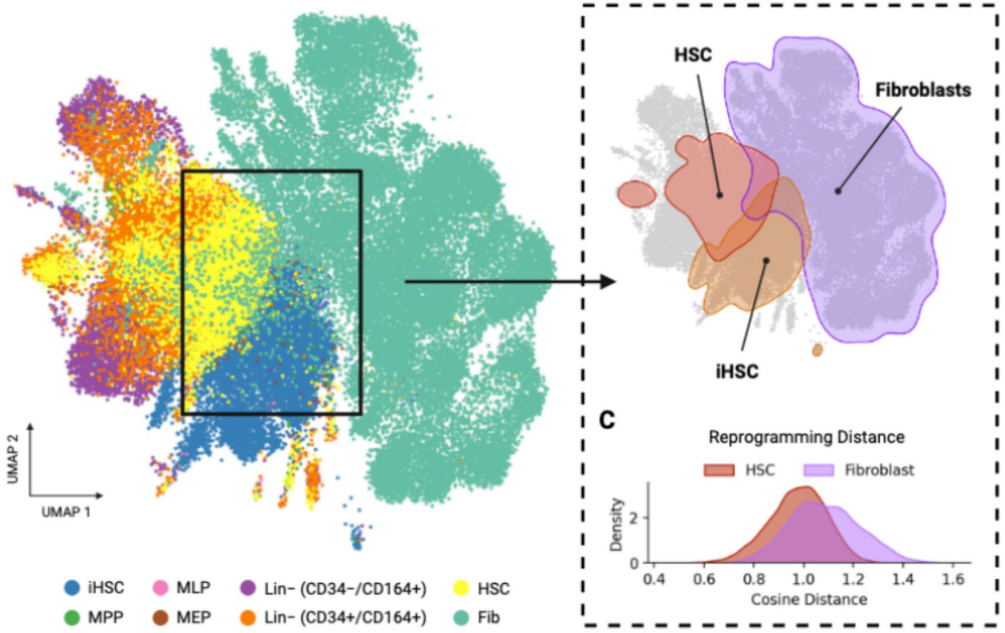

[1] Ronquist S, Patterson G, Muir LA, Lindsly S, Chen H, Brown M, Wicha M, Bloch A, Brockett R and Rajapakse I. "**Algorithm for Cellular Reprogramming.**" *Proceedings of the National Academy of Sciences* 114.45 (2017): 11832-11837.

Programmable Platform for Probing Cellular Dynamics

Automated Wound Healing Assay

Automated In Vitro Wound Healing Assay

Jillian Cwycyshyn[1, 2], Cooper Stansbury[2, 3], Walter Meixner[2], James B. Hoying[4], Lindsey A. Muir[2], and Indika Rajapakse[1, 2, 5]

[1]Department of Biomedical Engineering, University of Michigan, Ann Arbor, MI 48109 USA
[2]Department of Computational Medicine and Bioinformatics, University of Michigan, Ann Arbor, MI 48109 USA
[3]The Michigan Institute for Computational Discovery and Engineering, University of Michigan, Ann Arbor, MI 48109 USA
[4]Advanced Solutions Life Sciences, Manchester, NH 03101 USA
[5]Department of Mathematics, University of Michigan, Ann Arbor, MI 48109 USA

March 21, 2024

Abstract

Restoring the epidermal barrier after injury requires spatial and temporal orchestration of migration, proliferation, and signaling across many cell types. The mechanisms that coordinate this complex process are incompletely understood. In vitro wound assays are common model systems for examining these mechanisms in wound healing. In the scratch assay, a cell-free gap is created by mechanical removal of cells from a monolayer, followed by monitoring cell migration into the gap over time. While simple and low-cost, manual scratch assays are limited by low reproducibility and low throughput. Here, we have designed a robotics-assisted automated wound healing (AWH) assay that increases reproducibility and throughput while integrating automated live-cell imaging and analysis. Wounds are designed as computer-aided design (CAD) models and recreated in confluent cell layers by the BioAssemblyBot (BAB) 3D-bioprinting platform. The dynamics of migration and proliferation in individual cells are evaluated over the course of wound closure using live-cell fluorescence microscopy and our high-performance image processing pipeline. The AWH assay outperforms the standard scratch assay with enhanced consistency in wound geometry. Our ability to create diverse wound shapes in any multi-well plate with the BAB not only allows for multiple experimental conditions to be analyzed in parallel but also offers versatility in the design of wound healing experiments. Our method emerges as a valuable tool for the automated completion and analysis of high-throughput, reproducible, and adaptable in vitro wound healing assays.

Automated in vitro Wound Healing Assay

Robot-generated wounds

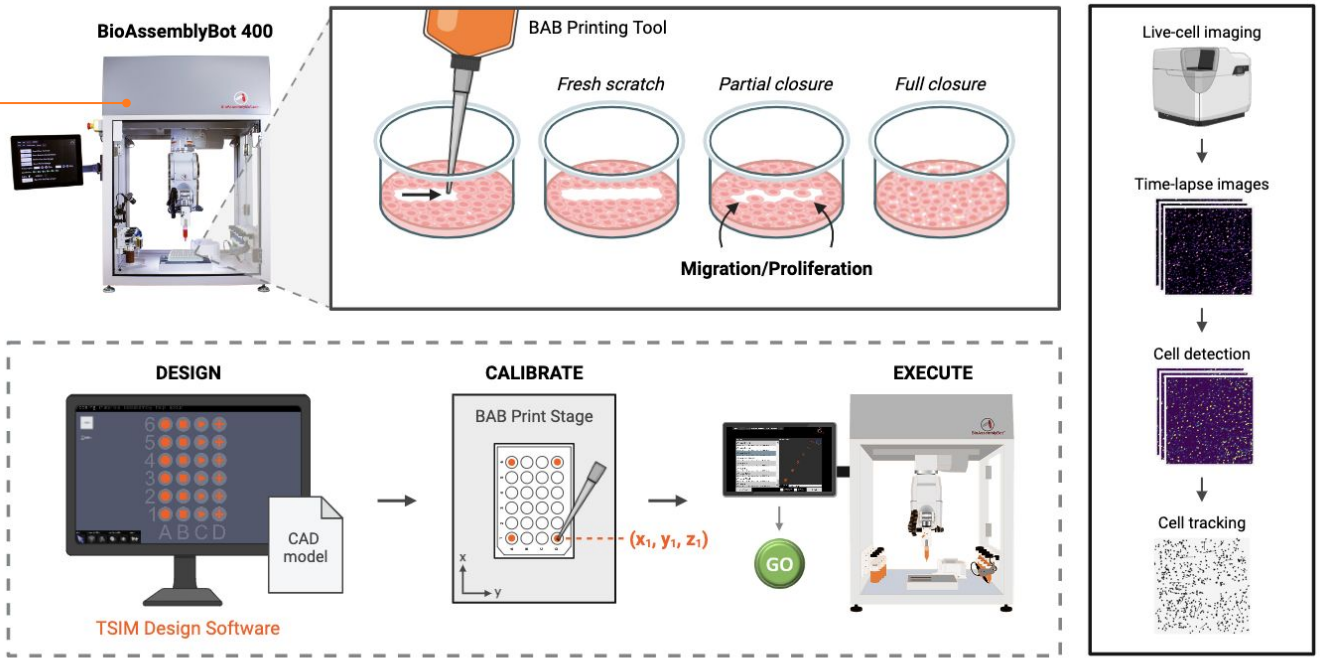

Any wound shape/size

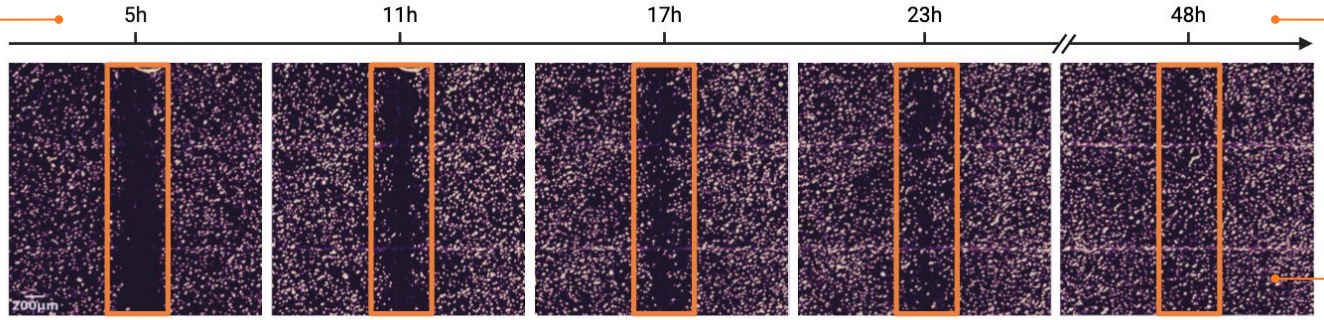

Cell tracking pipeline

Real-time monitoring

Jillian Cwycyshyn, Cooper Stansbury, Walter Meixner, James B. Hoying, Lindsey A. Muir, and Indika Rajapakse. **Automated In Vitro Wound Healing Assay.** APL Bioengineering, in revision

Data: Single Cell Pore-C (higher order structures in the genome)

Single Cell Hypergraphs and Hypergraph Core: Coming Soon

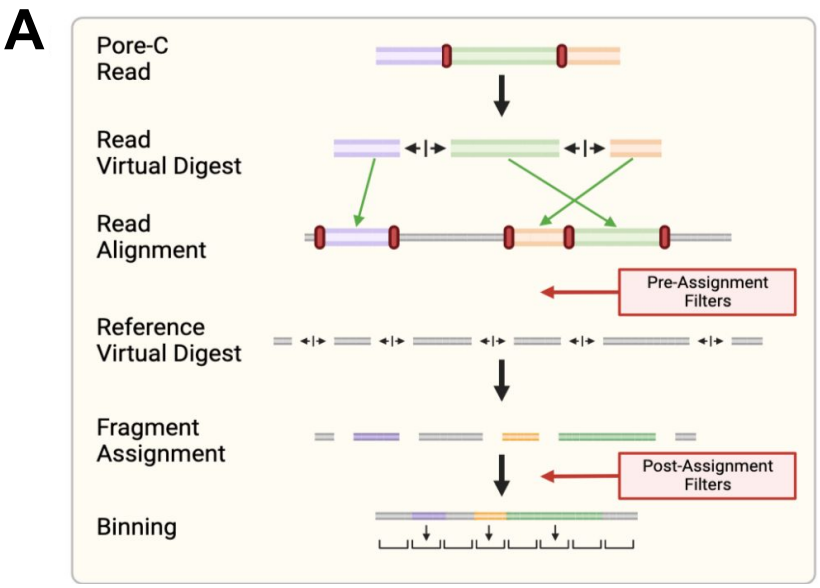

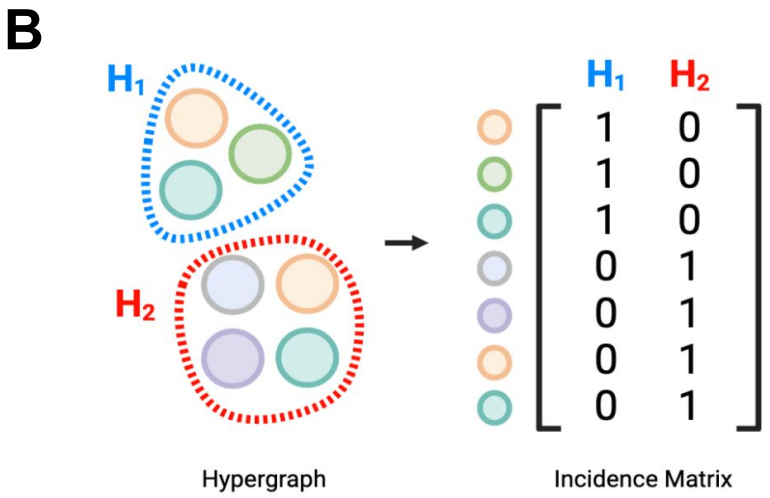

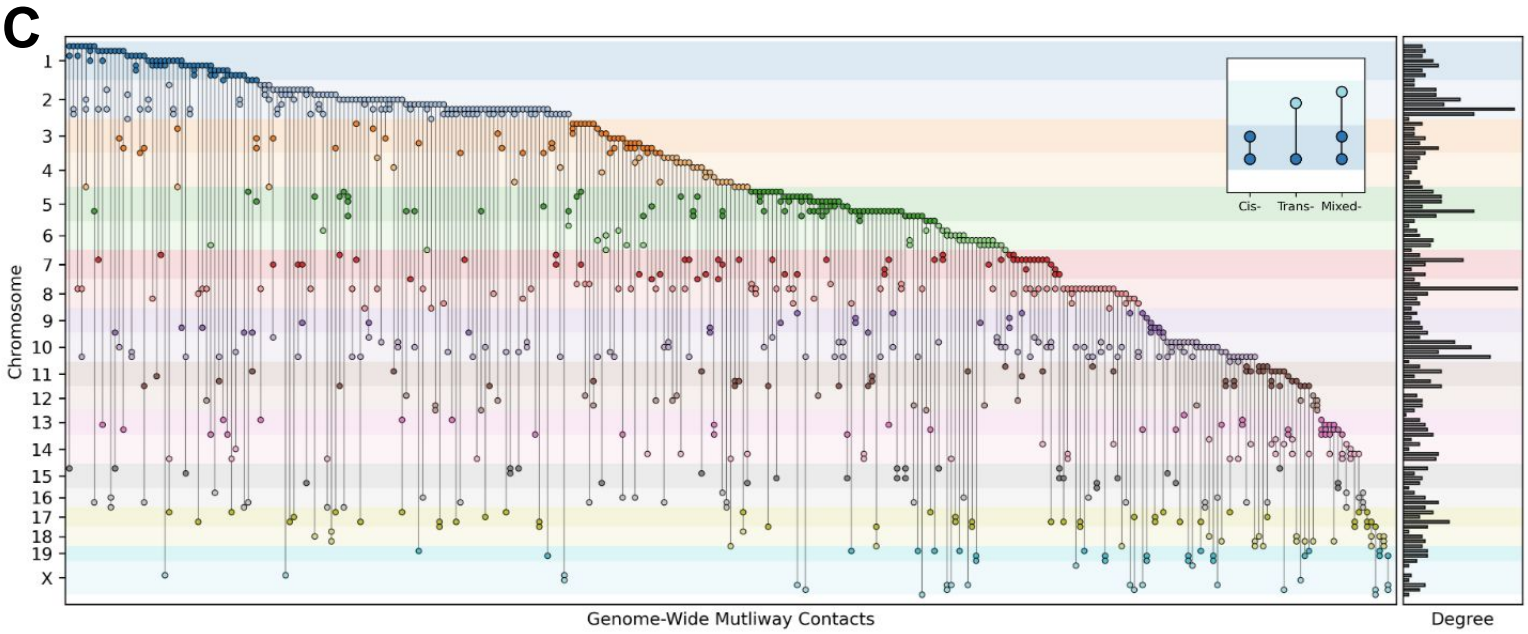

Large, Directed, Non-uniform Hypergraphs

$$\begin{cases} \dot{\mathbf{x}} &= \mathbf{f}(\mathbf{x}) = \mathbf{A}\mathbf{x}^{k-1} + \mathbf{B}\mathbf{u} \\ \mathbf{y} &= \mathbf{g}(\mathbf{x}) = \mathbf{C}\mathbf{x} \end{cases}$$

Tensor-based Evaluation

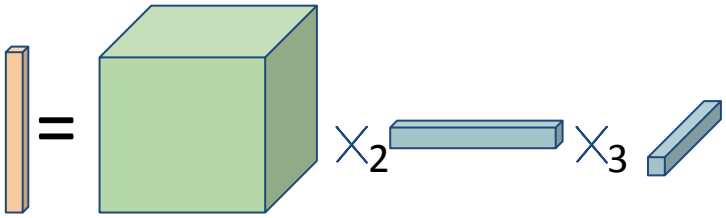

Matrix-based Evaluation

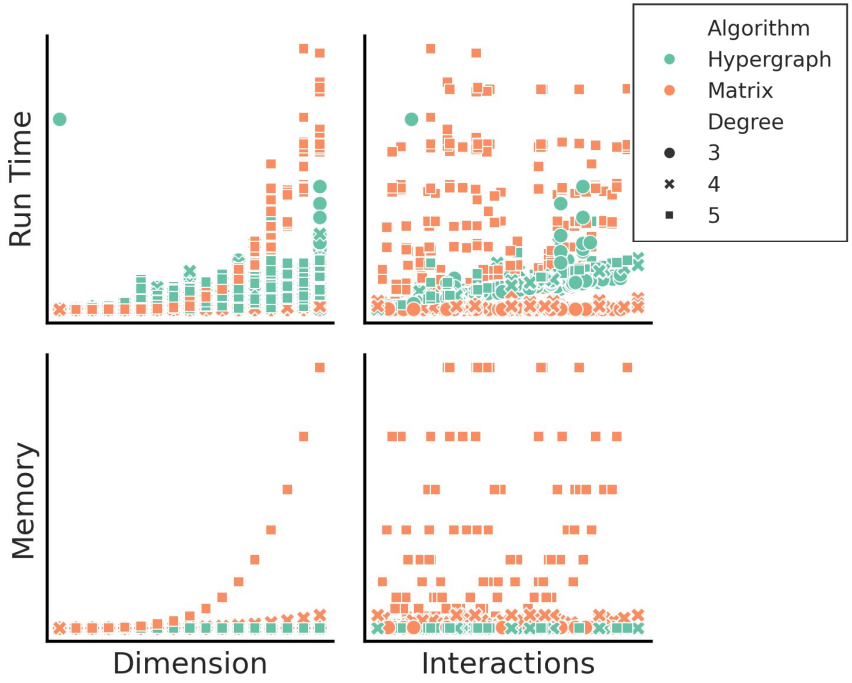

Hypergraph-based Evaluation

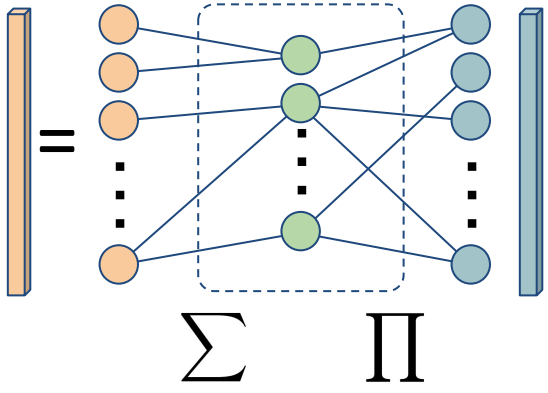

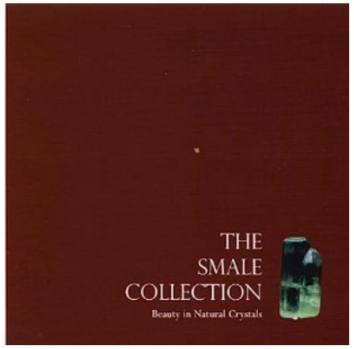

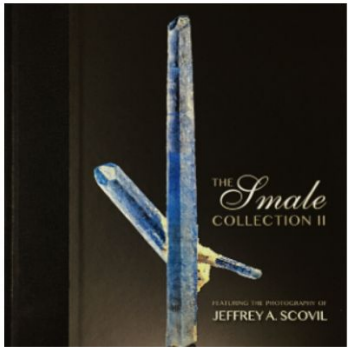

Virtual Museum

Smale 95

DATE: July 21 - 22, 2025

LOCATION: Simons Institute for the Theory of Computing, Berkeley, CA

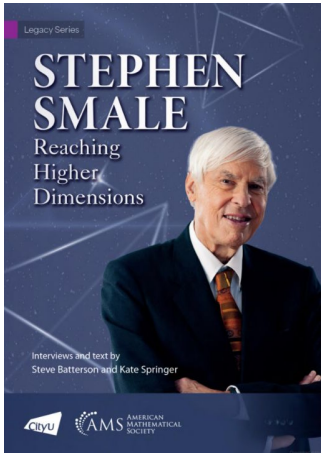

Thank you!

Ongoing and Future Directions

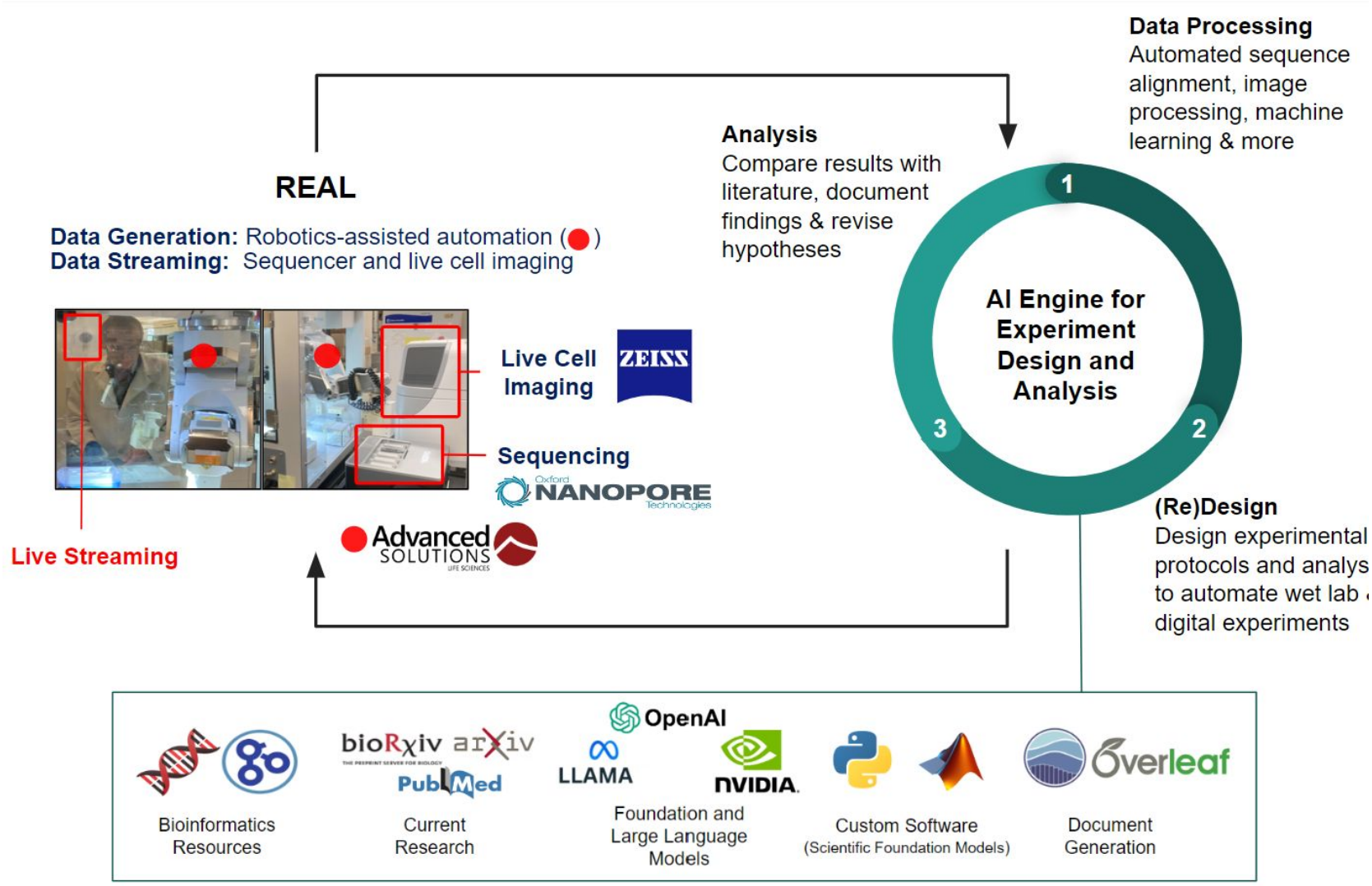

KRONECKER PRODUCT OF TENSORS AND HYPERGRAPHS: STRUCTURE AND DYNAMICS

JOSHUA PICKARD*, CAN CHEN†, COOPER STANSBURY‡, AMIT SURANA§, ANTHONY BLOCH¶, AND INDIKA RAJAPAKSE‖

Abstract. Hypergraphs and graph products extend traditional graph theory by incorporating multi-way and coupled relationships, which are ubiquitous in real-world systems. While the Kronecker product, rooted in matrix analysis, has become a powerful tool in network science, its application has been limited to pairwise networks. In this paper, we extend the coupling of graph products to hypergraphs, enabling a system-theoretic analysis of network compositions formed via the Kronecker product of hypergraphs. We first extend the notion of the matrix Kronecker product to the tensor Kronecker product from the perspective of tensor blocks. We present various algebraic and spectral properties and express different tensor decompositions with the tensor Kronecker product. Furthermore, we study the structure and dynamics of Kronecker hypergraphs based on the tensor Kronecker product. We establish conditions that enable the analysis of the trajectory and stability of a hypergraph dynamical system by examining the dynamics of its factor hypergraphs. Finally, we demonstrate the numerical advantage of this framework for computing various tensor decompositions and spectral properties.

Key words. Tensor Kronecker Product, hypergraph products, tensor decomposition, tensor eigenvalues, multilinear system, block tensors

AMS subject classifications. 15A69, 05C65

Accepted to SIMAX

KRONECKER PRODUCT OF TENSORS AND HYPERGRAPHS: STRUCTURE AND DYNAMICS

JOSHUA PICKARD*, CAN CHEN†, COOPER STANSBURY‡, AMIT SURANA§, ANTHONY BLOCH¶, AND INDIKA RAJAPAKSE‖

Abstract. Hypergraphs and graph products extend traditional graph theory by incorporating multi-way and coupled relationships, which are ubiquitous in real-world systems. While the Kronecker product, rooted in matrix analysis, has become a powerful tool in network science, its application has been limited to pairwise networks. In this paper, we extend the coupling of graph products to hypergraphs, enabling a system-theoretic analysis of network compositions formed via the Kronecker product of hypergraphs. We first extend the notion of the matrix Kronecker product to the tensor Kronecker product from the perspective of tensor blocks. We present various algebraic and spectral properties and express different tensor decompositions with the tensor Kronecker product. Furthermore, we study the structure and dynamics of Kronecker hypergraphs based on the tensor Kronecker product. We establish conditions that enable the analysis of the trajectory and stability of a hypergraph dynamical system by examining the dynamics of its factor hypergraphs. Finally, we demonstrate the numerical advantage of this framework for computing various tensor decompositions and spectral properties.

Key words. Tensor Kronecker Product, hypergraph products, tensor decomposition, tensor eigenvalues, multilinear system, block tensors

AMS subject classifications. 15A69, 05C65

Hypergraph Dynamics

Hypergraph dynamics are represented as homogeneous polynomial or multi-linear systems. A k-unifrom hypergraph $\mathcal{H}$ on with adjacency tensor A has the polynomial dynamics

$$\Sigma_H \begin{cases} \dot{\mathbf{x}} &= \mathrm{A}\mathbf{x}^{k-1} + \mathbf{Bu} \\ \mathbf{y} &= \mathbf{Cx} \end{cases}$$

with linear inputs and outputs.

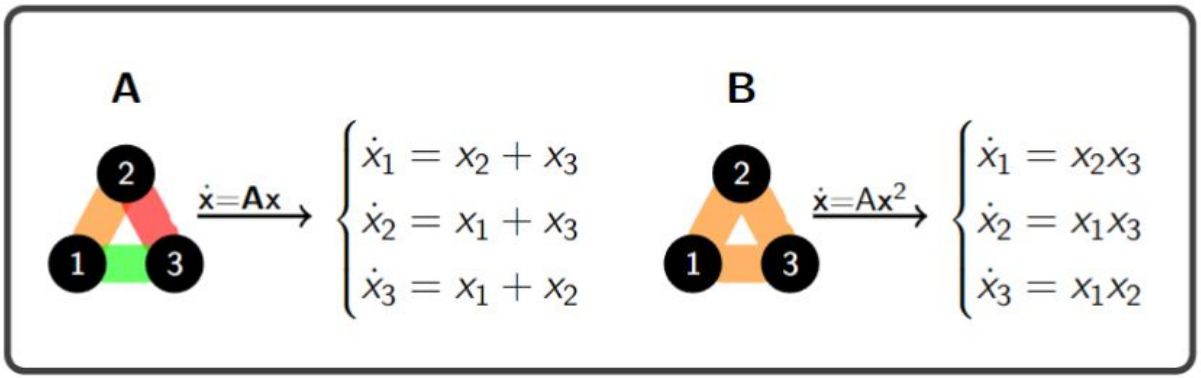

4

[4] Chen, Can, et al. "Controllability of hypergraphs." IEEE Transactions on Network Science and Engineering 8.2 (2021): 1646-1657.

Observability

A system is *observable* if the system state can be determined from the system output.

$$\Sigma_L \begin{cases} \dot{\mathbf{x}} &= \mathbf{A}\mathbf{x} + \mathbf{B}\mathbf{u} \\ \mathbf{y} &= \mathbf{C}\mathbf{x} \end{cases}$$

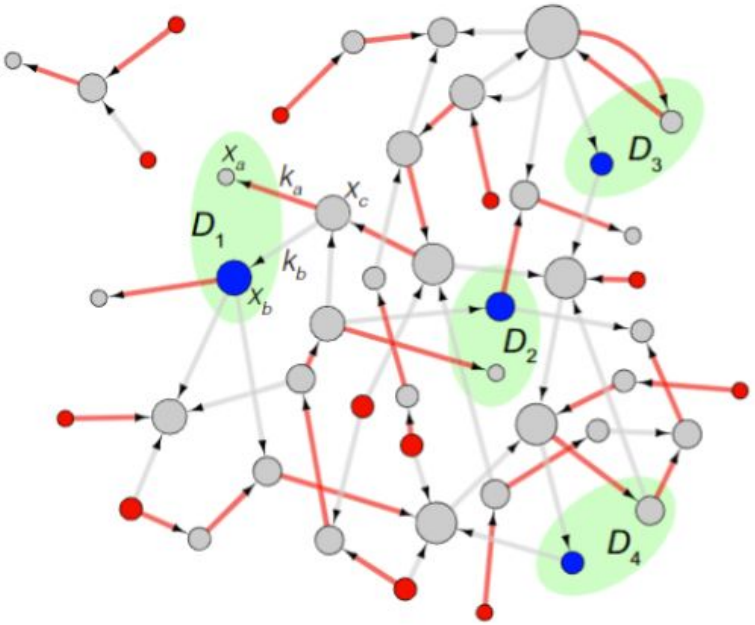

1

[1] Liu, Yang-Yu, Jean-Jacques Slotine, and Albert-László Barabási. "Observability of complex systems." Proceedings of the National Academy of Sciences 110.7 (2013): 2460-2465.

Hypergraph Dynamics

Repeated Kronecker Product

$$\mathbf{x}^{[i]} = \underbrace{\mathbf{x} \otimes \mathbf{x} \cdots \otimes \mathbf{x}}_{i-\text{times}}.$$

Hypergraph dynamics without control:

$$\Sigma_H \begin{cases} \dot{\mathbf{x}} &= A\mathbf{x}^{k-1} \\ \mathbf{y} &= \mathbf{C}\mathbf{x} \end{cases} \xrightarrow{\text{Tensor Unfolding}} \Sigma_H \begin{cases} \dot{\mathbf{x}} &= A_{(p)}\mathbf{x}^{[k-1]} \\ \mathbf{y} &= \mathbf{C}\mathbf{x} \end{cases}$$

$$\xrightarrow{\text{Nonlinear System}} \Sigma_N \begin{cases} \dot{\mathbf{x}} &= \mathbf{f}(\mathbf{x}) \\ \mathbf{y} &= \mathbf{g}(\mathbf{x}) \end{cases}$$

Nonlinear Observability Matrix (NOM)

Kalman-like Observability Test

When $rank(\mathcal{O}(\mathbf{x})) = dim(\mathbf{x})$, the system is locally, weakly observable.

$$\mathcal{O} = \begin{pmatrix} \mathbf{C} \\ \mathbf{CA} \\ \mathbf{CA}^2 \\ \vdots \\ \mathbf{CA}^{n-1} \end{pmatrix} \approx \begin{pmatrix} \mathbf{y} \\ \frac{d\mathbf{y}}{dt} \\ \frac{d^2\mathbf{y}}{dt^2} \\ \vdots \\ \frac{d^{n-1}\mathbf{y}}{dt^{n-1}} \end{pmatrix} \xrightarrow{Nonlinear} \mathcal{O}(\mathbf{x}) = \nabla_{\mathbf{x}} \begin{pmatrix} L_{\mathbf{f}}^0\mathbf{g}(\mathbf{x}) \\ L_{\mathbf{f}}^1\mathbf{g}(\mathbf{x}) \\ \vdots \\ L_{\mathbf{f}}^r\mathbf{g}(\mathbf{x}) \end{pmatrix} \quad (4)$$

Nonlinear Observability Matrix (NOM)

Kalman-like Observability Test

When $rank(\mathcal{O}(\mathbf{x})) = dim(\mathbf{x})$, the hypergraph dynamics are locally, weakly observable.

$$\mathcal{O}(\mathbf{x}) = \nabla_{\mathbf{x}} \begin{pmatrix} L_{\mathbf{f}}^{0}\mathbf{g}(\mathbf{x}) \\ L_{\mathbf{f}}^{1}\mathbf{g}(\mathbf{x}) \\ \vdots \\ L_{\mathbf{f}}^{r}\mathbf{g}(\mathbf{x}) \end{pmatrix} = \nabla_{\mathbf{x}} \begin{pmatrix} \mathbf{C}\mathbf{x} \\ \mathbf{C}\mathbf{A}\mathbf{x}^{[k-1]} \\ \mathbf{C}\mathbf{A}\mathbf{B}_2\mathbf{x}^{[2k-3]} \\ \vdots \\ \mathbf{C}\mathbf{A}\mathbf{B}_2 \ldots \mathbf{B}_n\mathbf{x}^{[nk-(2n-1)]} \end{pmatrix} \tag{5}$$

$$\mathbf{B}_p = \sum_{i=1}^{(p-1)k-(2p-3)} \overbrace{\mathbf{I} \otimes \cdots \otimes \underbrace{\mathbf{A}_{(p)}}_{i\text{-th pos.}} \otimes \cdots \otimes \mathbf{I}}^{(p-1)k-(2p-3)\text{times}}$$

See Sontag, Krener and Baillieul

Computing the Hypergraph Nonlinear Observability Matrix

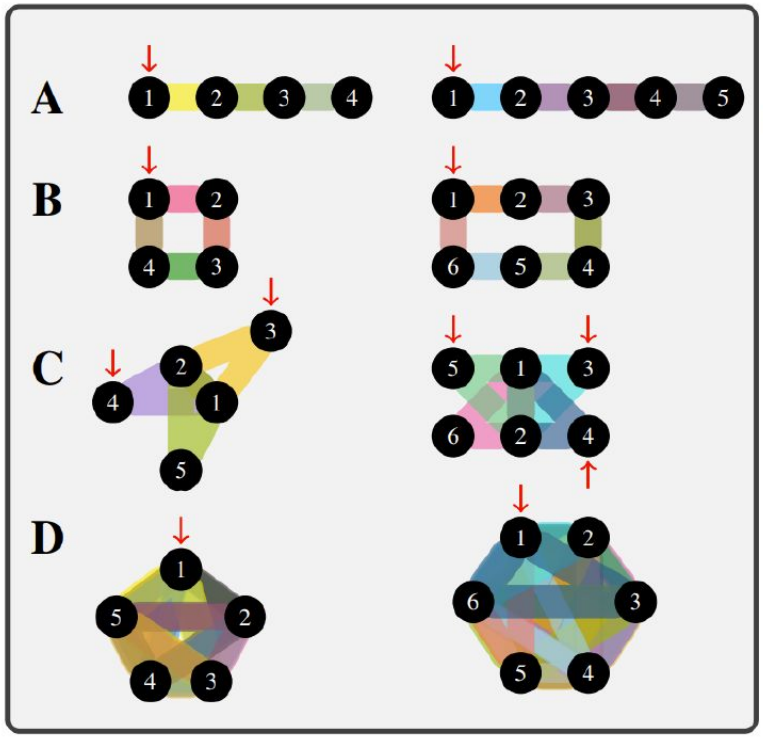

Algorithm 1 A recursive algorithm for computing $\mathbf{L_h(g)}$

1: **RecursiveL**$(\mathbf{C}, \mathbf{A},\ p,\ k, S_j)$
2: **if** $p = 1$ **then**
3: $\quad L_h(g(\mathbf{x})) = \mathbf{CA}\left(S_{j,1} \otimes \cdots \otimes S_{j,(k-1)}\right)$
4: $\quad$ **return:** $L_h(g(\mathbf{x}))$
5: **end if**
6: $b = (p-1)k - (2p-3)$
7: $L_h(g(\mathbf{x})) = 0$
8: **for** $i = 1, \ldots, b$ **do**
9: $\quad S_i' = \{S_{j,1}, \ldots, \overbrace{\mathbf{A}\left(S_{j,i} \otimes \cdots \otimes S_{j,i+k-2}\right)}^{i\text{th pos.}}, \ldots, S_{j,pk-(2p-1)}\}$
10: $\quad L_h(g(\mathbf{x})) = L_h(g(\mathbf{x})) + \mathbf{RecursiveL}(\mathbf{C}, \mathbf{A},\ p-1, k, S_i')$
11: **end for**
12: **return:** $L_h(g(\mathbf{x}))$

Symbolic Calculations

Hypergraph controllability has been studied similarly

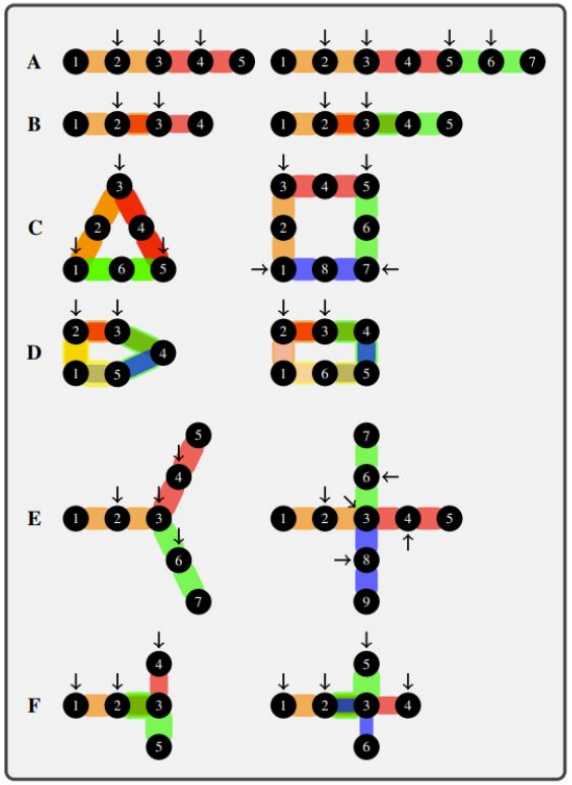

Algorithm 1 Computing the reduced controllability matrix.

1: Given a supersymmetric tensor $\mathsf{A} \in \mathbb{R}^{n \times n \times \cdots \times n}$ and a control matrix $\mathbf{B} \in \mathbb{R}^{n \times m}$
2: Unfold A into a matrix $\mathbf{A}$ by stacking the last $k-1$ modes, i.e., $\mathbf{A} \in \mathbb{R}^{n \times n^{k-1}}$
3: Set $\mathbf{C}_r = \mathbf{B}$ and $j = 0$
4: **while** $j < n$ **do**
5: Compute $\mathbf{L} = \mathbf{A}(\mathbf{C}_r \otimes \mathbf{C}_r \otimes \overset{k-1}{\cdots} \otimes \mathbf{C}_r)$
6: Set $\mathbf{C}_r = \begin{bmatrix} \mathbf{C}_r & \mathbf{L} \end{bmatrix}$
7: Compute the economy-size SVD of $\mathbf{C}_r$, and remove the zero singular values, i.e., $\mathbf{C}_r = \mathbf{U}\mathbf{S}\mathbf{V}^\top$ where $\mathbf{S} \in \mathbb{R}^{s \times s}$, and s is the rank of $\mathbf{C}_r$
8: Set $\mathbf{C}_r = \mathbf{U}$, and $j = j + 1$
9: **end while**
10: **return** The reduced controllability matrix $\mathbf{C}_r$.

[5]

[5] Chen, Can, et al. "Controllability of hypergraphs." IEEE Transactions on Network Science and Engineering 8.2 (2021): 1646-1657.

Better than Graph Observability

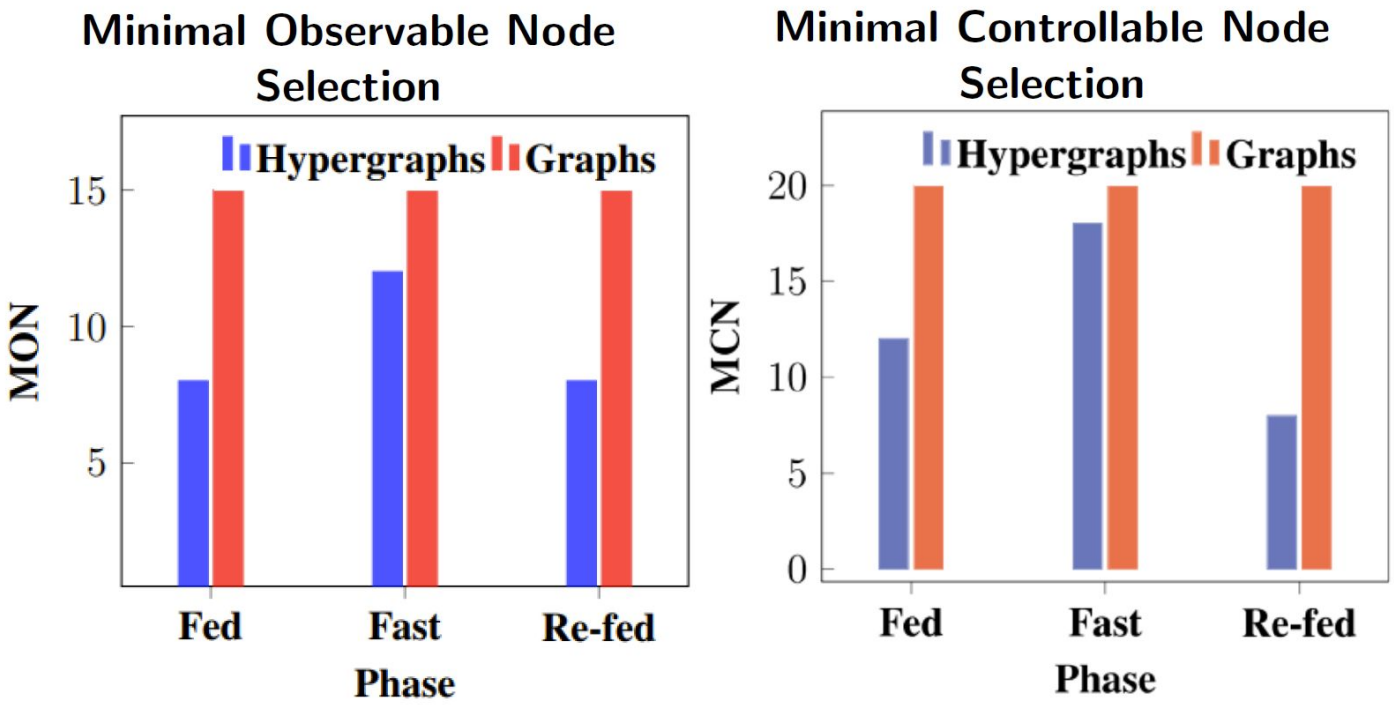

6

[6] Chen, Can, et al. "Controllability of hypergraphs." IEEE Transactions on Network Science and Engineering 8.2 (2021): 1646-1657.

DATA

Sweeney P, Chen C, Rajapakse I, Cone R. "Network Dynamics of Hypothalamic Feeding Neurons." *Proceedings of the National Academy of Sciences*, 118.14

Systems of Systems

Stochastic Kronecker Graph

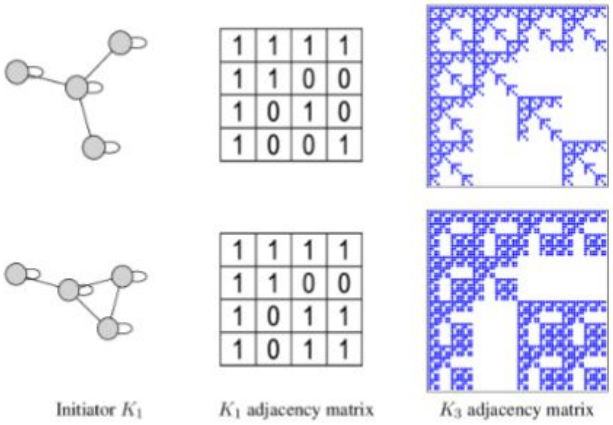

Tensor Kronecker Product

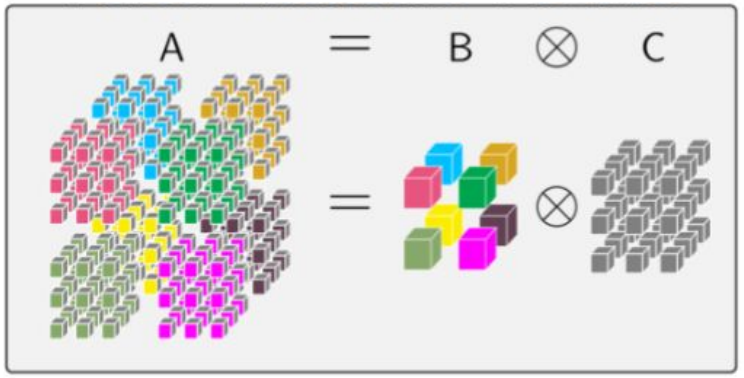

Tensor Decompositions

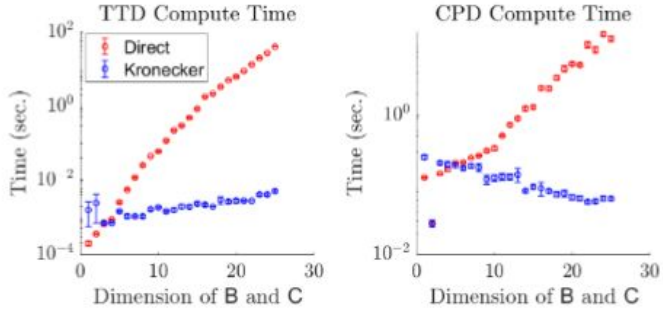

8

[8] (Left) Leskovec, Jure, et al. "Kronecker graphs: an approach to modeling networks." Journal of Machine Learning Research 11.2 (2010).

KRONECKER PRODUCT OF TENSORS AND HYPERGRAPHS: STRUCTURE AND DYNAMICS

JOSHUA PICKARD*, CAN CHEN†, COOPER STANSBURY‡, AMIT SURANA§, ANTHONY BLOCH¶, AND INDIKA RAJAPAKSE‖

Abstract. Hypergraphs and graph products extend traditional graph theory by incorporating multi-way and coupled relationships, which are ubiquitous in real-world systems. While the Kronecker product, rooted in matrix analysis, has become a powerful tool in network science, its application has been limited to pairwise networks. In this paper, we extend the coupling of graph products to hypergraphs, enabling a system-theoretic analysis of network compositions formed via the Kronecker product of hypergraphs. We first extend the notion of the matrix Kronecker product to the tensor Kronecker product from the perspective of tensor blocks. We present various algebraic and spectral properties and express different tensor decompositions with the tensor Kronecker product. Furthermore, we study the structure and dynamics of Kronecker hypergraphs based on the tensor Kronecker product. We establish conditions that enable the analysis of the trajectory and stability of a hypergraph dynamical system by examining the dynamics of its factor hypergraphs. Finally, we demonstrate the numerical advantage of this framework for computing various tensor decompositions and spectral properties.

Key words. Tensor Kronecker Product, hypergraph products, tensor decomposition, tensor eigenvalues, multilinear system, block tensors

AMS subject classifications. 15A69, 05C65

Data from the LAB

Cell Dynamics

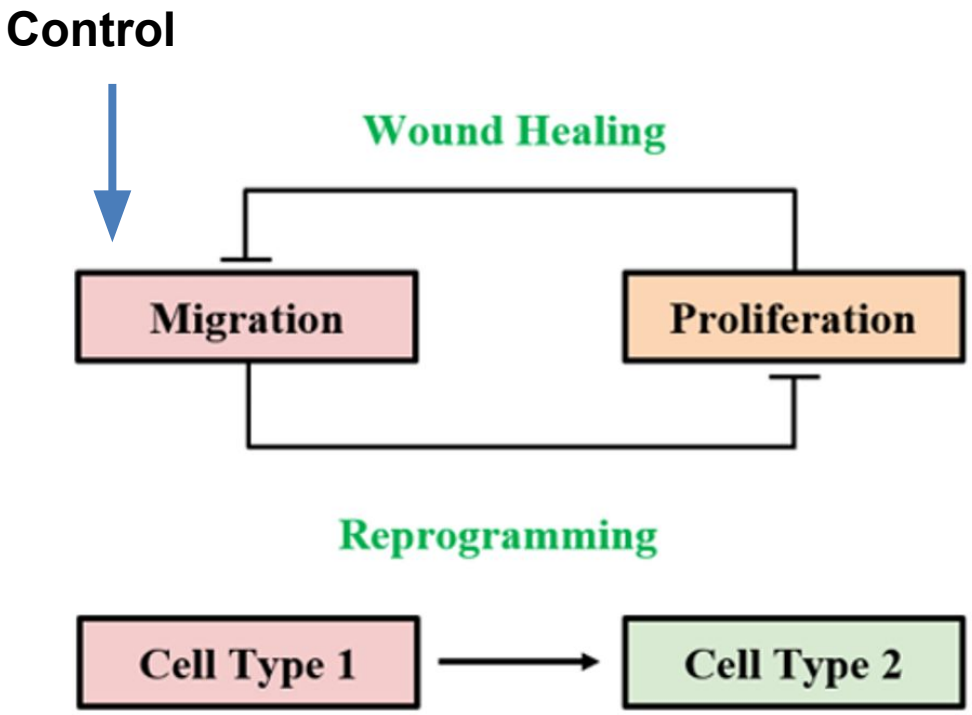

Biology of Wound Healing

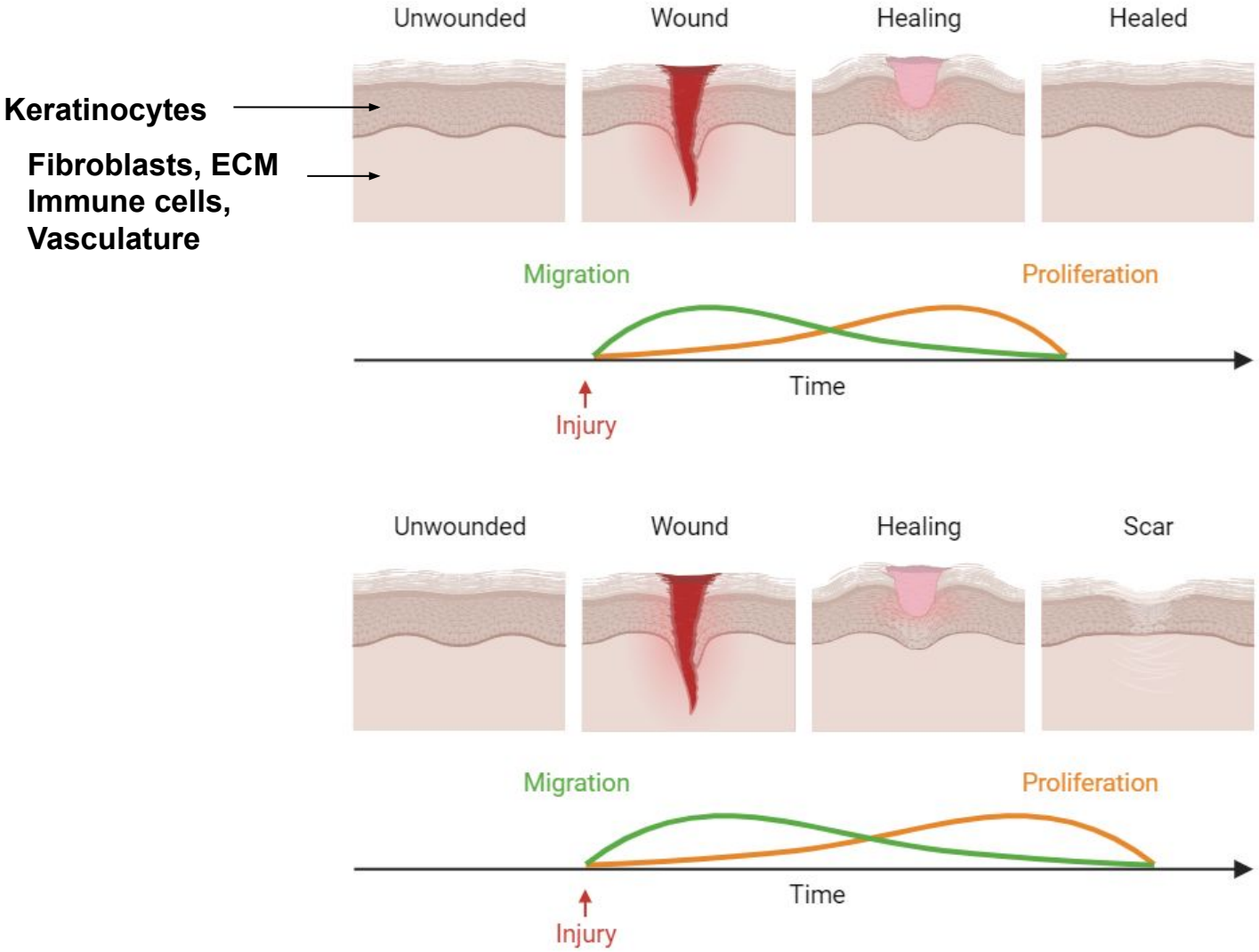

Wound Healing System: In Vitro Analog

Fibroblasts (nucleus) | Keratinocytes | Fibroblasts | Composite

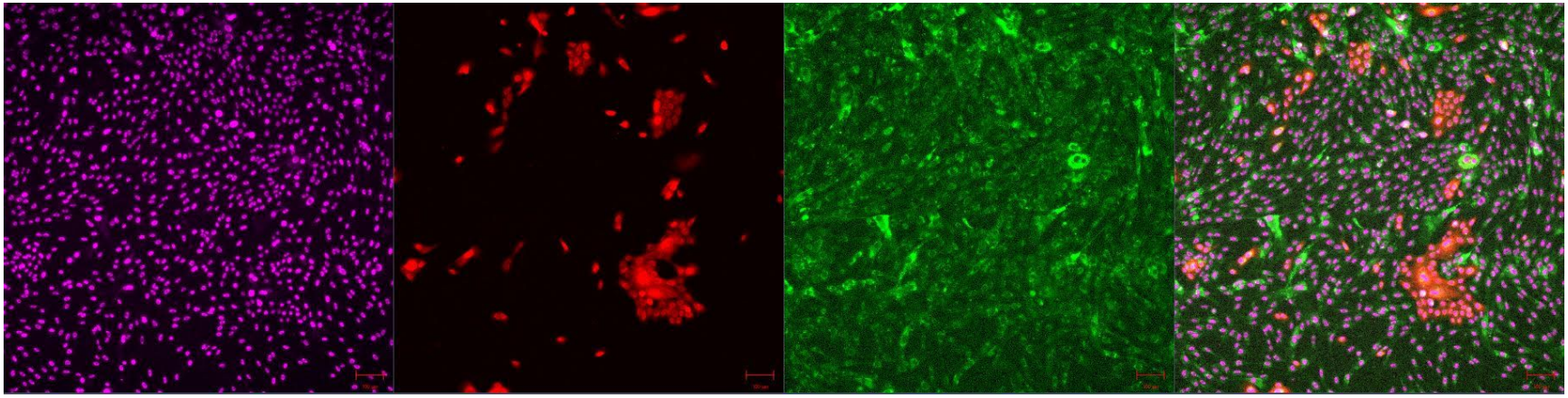

Wound

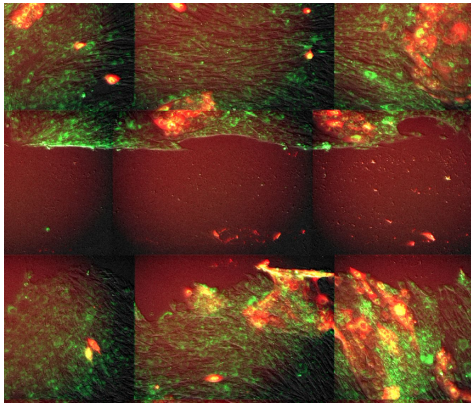

Healing

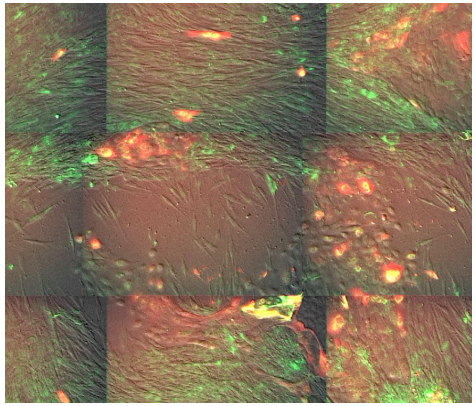

Next Generation

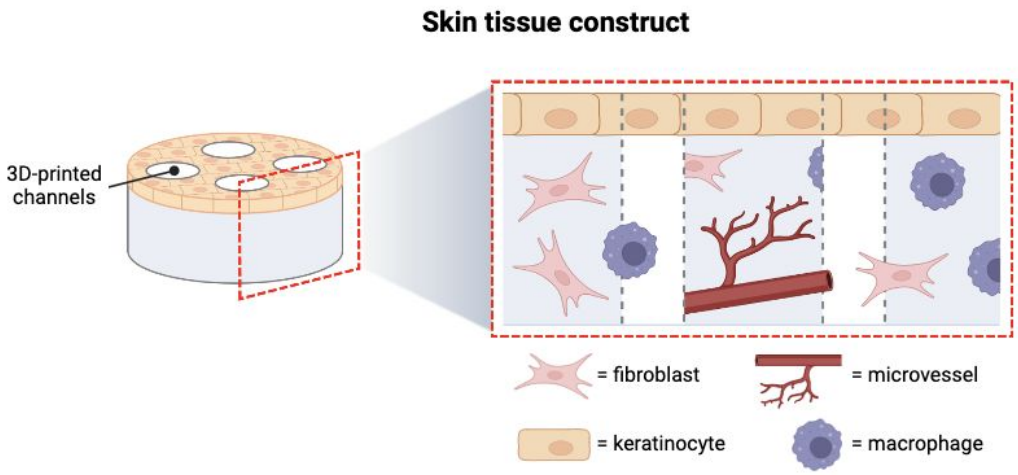

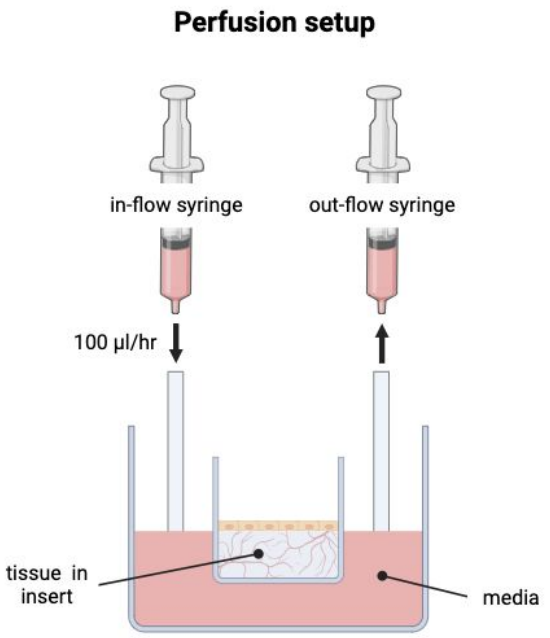

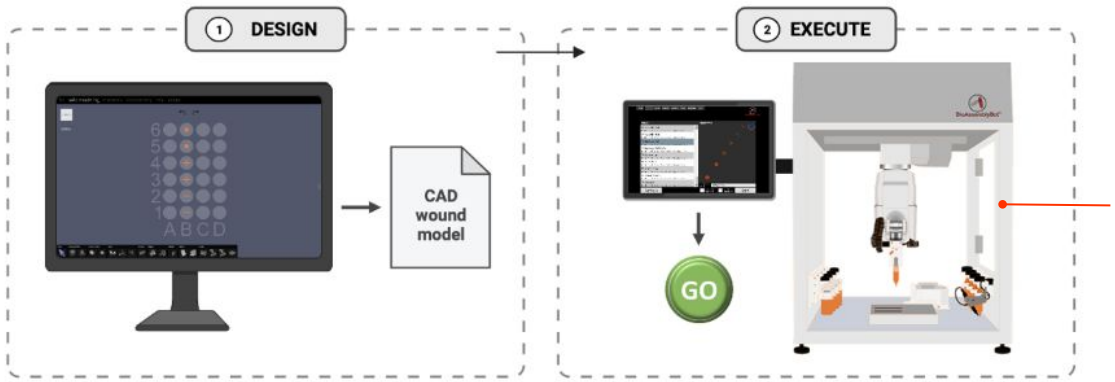

The BioAssemblyBot 400 (BAB)

Automation

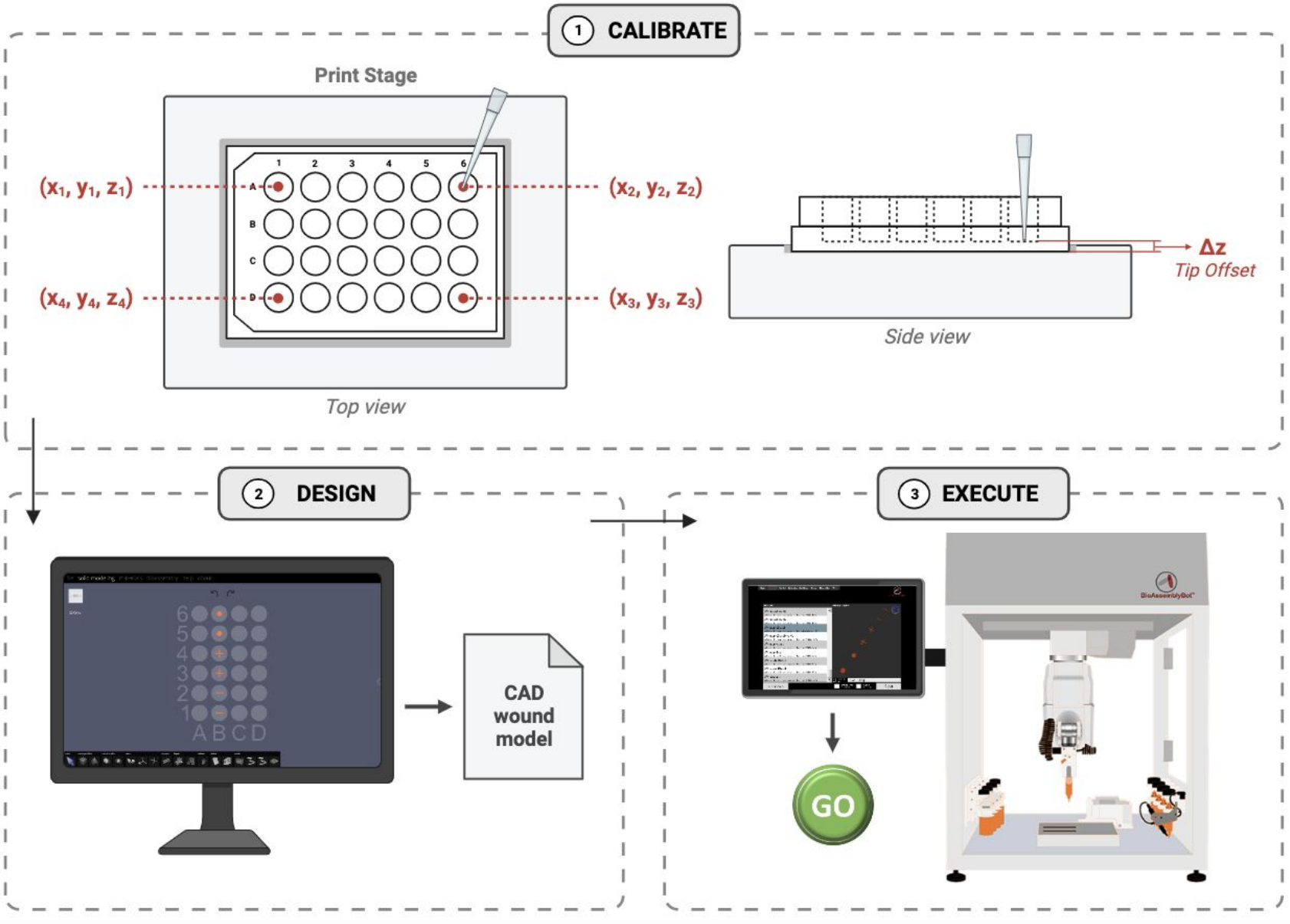
1 CALIBRATE
Print Stage
(x1, y1, z1)
(x2, y2, z2)
(x4, y4, z4)
(x3, y3, z3)
Top view
Δz
Tip Offset
Side view
2 DESIGN
CAD wound model
3 EXECUTE
GO

LAB 2023: Technology

Oxford Nanopore Sequencing

MinION

GridION

PromethION 2

The BAB robotic arm

BAB Pick n' Place tool (i.e., the grippers)

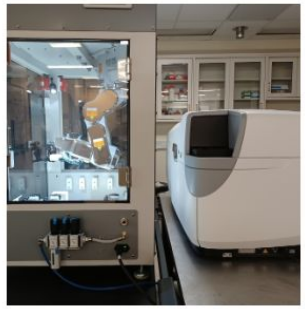

The BAB and Zeiss Celldiscoverer 7

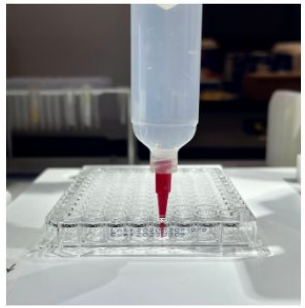

BAB Printing Tool used to automate a wound healing assay

University Research Instrumentation Program (DURIP), 2019 and 2022
Air Force Office of Scientific Research (Dr. Fred Leve)








Industrial Collaborators

Jay Hoying
Advanced Solutions

Lakmal Jayasinghe
Oxford Nanopore Technologies

Amit Surana
Raytheon Technologies

Technology Transfer to Startup: iReprogram Inc.

Automation in the LAB

Live Cell Imaging

BAB

ONT Sequencer

Live Streaming

Thank you!

Scaling Hypergraph Observability Calculations

Tensor-based Evaluation

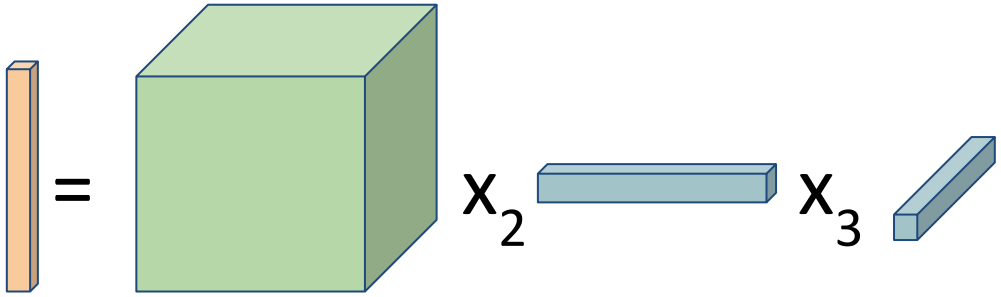

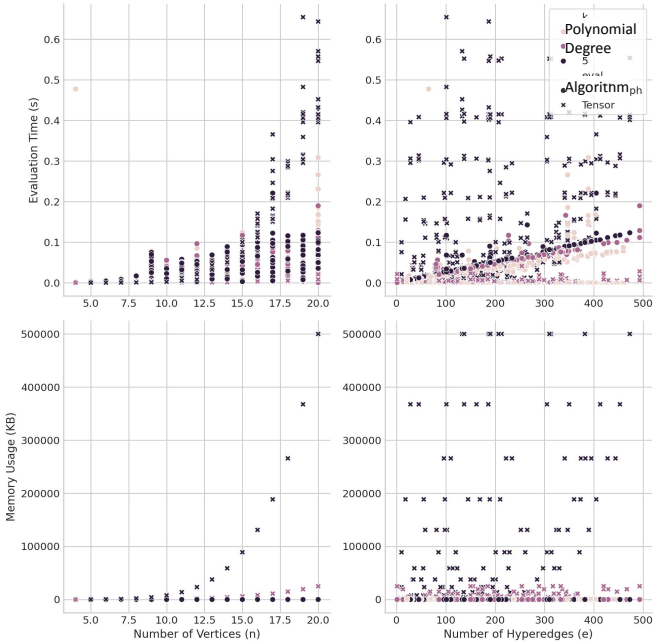

Matrix-based Evaluation

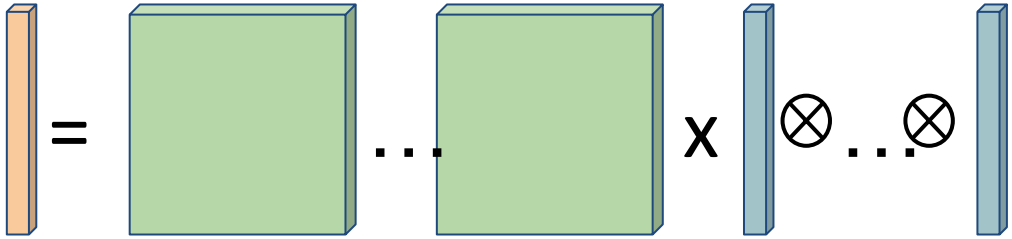

Hypergraph-based Evaluation

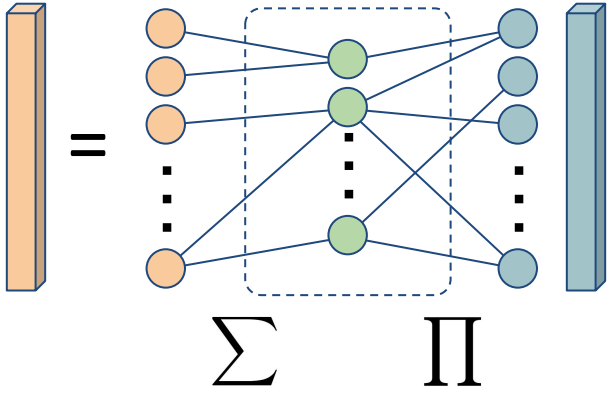

Algorithm 1 Hypergraph based evaluation of $\mathbf{f}(\mathbf{x})$

Require: $\mathcal{H}$: list of hyperedges, $\mathbf{x}$: vector of node states
Ensure: Updated vector of node states
1: Initialize $\mathbf{x}' \leftarrow [0, 0, \ldots, 0]$ of length $|\mathbf{x}|$
2: **for all** $h \in \mathcal{H}$ **do**
3: Let $polyterm \leftarrow \prod_{v \in \text{tail}(h)} \mathbf{x}[v]$
4: $\mathbf{x}'[\text{head}(h)] \leftarrow \mathbf{x}'[\text{head}(h)] + polyterm$
5: **end for**
6: **return** $\mathbf{x}'$

Large, Directed, Non-uniform Hypergraphs

$$\begin{cases} \dot{\mathbf{x}} &= \mathbf{f}(\mathbf{x}) = \mathbf{A}\mathbf{x}^{k-1} + \mathbf{B}\mathbf{u} \\ \mathbf{y} &= \mathbf{g}(\mathbf{x}) = \mathbf{C}\mathbf{x} \end{cases}$$

Tensor-based Evaluation

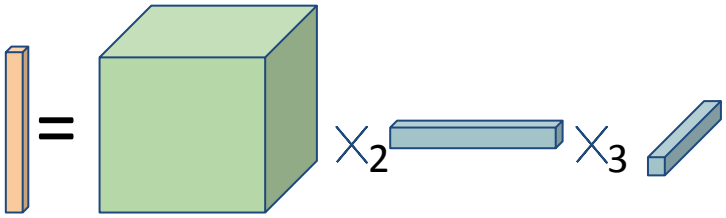

Matrix-based Evaluation

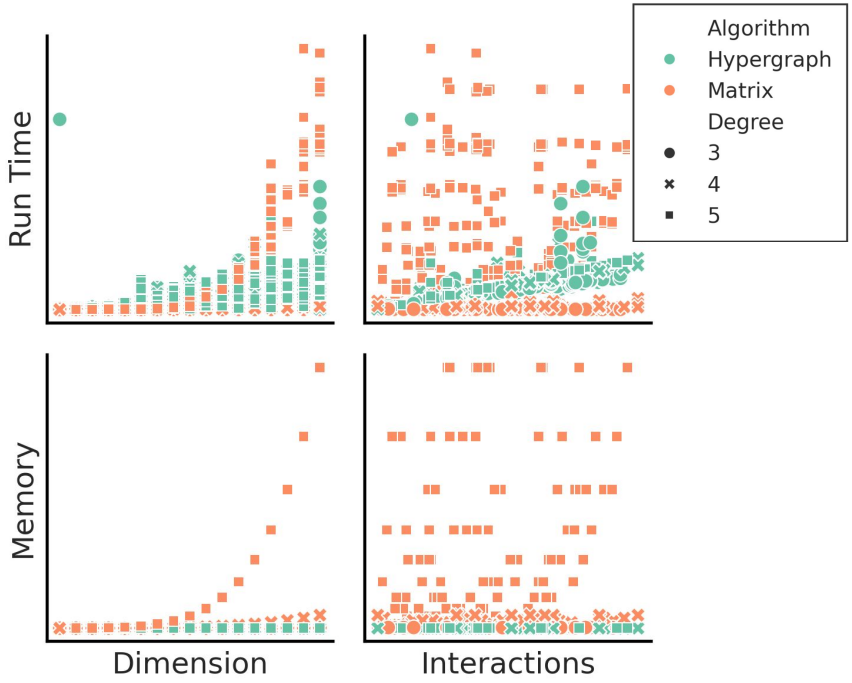

Hypergraph-based Evaluation

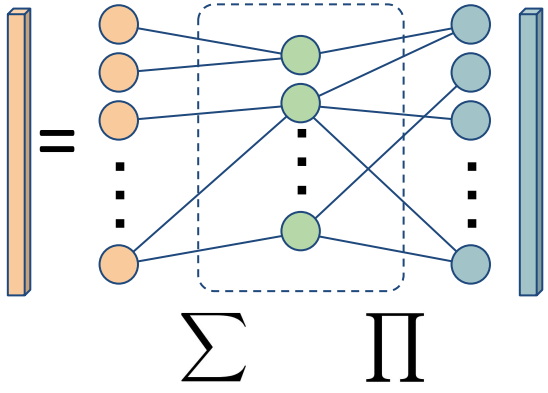

Tensor-based Evaluation

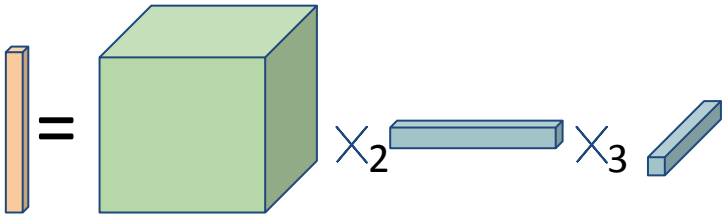

Matrix-based Evaluation

Hypergraph-based Evaluation

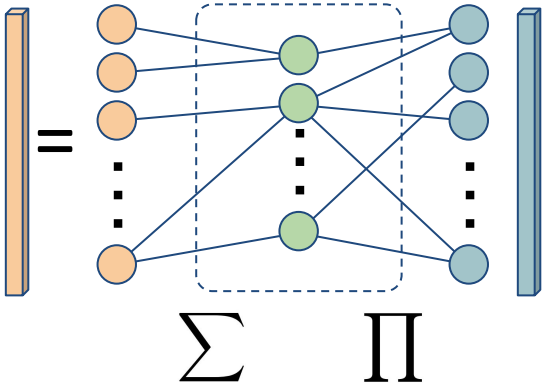

Numerical Comparison